

EXPERIMENTAL INVESTIGATION THE
EFFECT OF NANOFUID ON THE PRESSURE
DROP ACROSS THE SOLAR COLLECTOR

NURSHAHIERA BINTI MOHIDIN

BACHELOR OF ENGINEERING
UNIVERSITI MALAYSIA PAHANG

EXPERIMENTAL INVESTIGATION THE EFFECT OF NANOFUID ON THE
PRESSURE DROP ACROSS THE SOLAR COLLECTOR

NURSHAHIERA BINTI MOHIDIN

Report submitted in partial fulfillment of the
requirements for the award of the degree of
Bachelor of Mechanical Engineering

Faculty of Mechanical Engineering
UNIVERSITI MALAYSIA PAHANG

JUNE 2013

UNIVERSITI MALAYSIA PAHANG
FACULLTY OF MECHANICAL ENGINEERING

I certify that the project entitle “Experiment investigation the effect of nanofluid on the pressure drop across the solar collector” is written by Nurshahiera Binti Mohidin. I have examined the final copy of this project and in my opinion; it is fully adequate in terms of language standard and report formatting requirement for the award of the degree of Bachelor of Engineering. I herewith recommend that it be accepted in partial fulfillment of the requirements for the degree of Bachelor of Mechanical Engineering.

DR GAN LEONG MING

Examiner

Signature

SUPERVISOR'S DECLARATION

I hereby declare that I have checked this project and in my opinion, this project is adequate in terms of scope and quality for the award of the degree of Bachelor of Mechanical Engineering.

Signature

Name of supervisor: LEE GIOK CHUI KMN., SMP

Position: LECTURER OF FACULTY OF MECHANICAL ENGINEERING

Date: 4 JUNE 2013

STUDENT'S DECLARATION

I hereby declare that the work in this project is my own except for quotations and summarise which have been duly acknowledge. The project has not been accepted for any degree and its not concurrently submitted for award of other degree.

Signature:

Name: NURSHAHIERA BINTI MOHIDIN

ID Number: MA09027

Date: 4 JUNE 2013

**I specially dedicate to my parents and those who have guided and movitated me
for this project.**

ACKNOWLEDGEMENT

All the way through the development of this project I have learnt new skills and knowledge about the renewable energy especially the solar energy. I wish to express my sincere appreciation and gratitude to my supervisor, Mr lee Giok Chui for his continuous guidance, concern, encouragement and advice which gave me much inspiration in accomplishing my final project.

Special thanks to Mahendran a/l Moorthy for supporting and give continuous guidance to me in accomplishing my final year project.

My sincere gratitude to the lectures of Faculty of Mechanical Engineering who have put in effort to the lectures and always nurture and guide us with precious advices.

Last but not least, thanks to my dearly loved family members and friends who always help me in my studies.

ABSTRACT

This is a study on the performance of a pressure drop system of a evacuated tube solar collector. The objective of this project is to analysis the effect of nanofluid as the working fluid and temperature on the pressure drop by determining the pressure drop by using distilled water and nanofluid at different flow rate. The existing solar system installed in UMP Pekan does not measure the pressure drop. Various working fluid and mass flow rate was use in order to measure pressure drop. The experiment is conducted at solar system installed at UMP Pekan and the data is collected at three hour time interval which is at 9 am, 12 pm and 3 pm. The data analysed using the theoretical analysis and plotted in graph to discuss about it. The pressure drop obtained for nanofluid in this experiment is higher than distilled water. The minimum pressure drop within this experiment for distilled water and nanofluid is 694 Pa and 989 Pa respectively. The maximum pressure drop within this experiment for distilled water and nanofluid is 2336 Pa and 2390 Pa respectively. The pressure drop increase as the temperature increase. Within in this experiment for both working fluid the pressure drop is lowest at 9 am which is at that time temperature is the lowest. Although all the above findings refer to a particular flow rate which is for flow rate 2 , 2.5, 3.0, 3.5 litre/min, the better results can be obtained if the flow rate is varied. Finally by considering the problem of accuracy of the result, pressure transducer should be used instead of used manometer to measure the pressure drop.

ABSTRAK

Ini adalah satu kajian terhadap prestasi sistem perubahan tekanan di dalam tiub sistem pengumpul suria. Objektif projek ini adalah untuk analisis kesan nanofluid sebagai bendalir kerja yang digunakan dan suhu dengan menentukan perubahan tekanan dengan menggunakan air suling dan nanofluid pada kadar aliran yang berbeza. Sistem solar yang sedia ada dipasang di UMP Pekan tidak mengukur kejatuhan tekanan. Pelbagai bendalir kerjaa kadar aliran digunakan untuk mengukur perubahan tekanan. Eksperimen telah dijalankan di sistem solar yang dipasang di UMP Pekan dan data dikumpul pada jam 9 pagi, 12 tengah hari dan 3 petang. Data dianalisis dengan menggunakan analisis teori dan diplot dalam graf untuk membincangkan mengenainya. Perubahan tekanan yang diperolehi untuk nanofluid dalam eksperimen ini adalah lebih tinggi daripada air suling. Perubahan tekanan minimum dalam eksperimen ini untuk air suling dan nanofluid adalah 694 dan 989 Pa. Peningkatan perubahan tekanan adalah disebabkan oleh kenaikan suhu. Dalam eksperimen ini untuk kedua-dua bendalir bekerja perubahan tekanan paling rendah pada pukul 9 pagi iaitu pada suhu paling rendah. Walaupun semua dapatan di atas merujuk kepada kadar aliran tertentu iaitu pada kadar aliran 2, 2.5, 3.0, 3.5 liter / min, keputusan yang lebih baik boleh diperolehi jika kadar aliran yang lebih bayak digunakan. Akhirnya dengan mempertimbangkan masalah ketepatan keputusan, transduser tekanan perlu digunakan berbanding menggunakan manometer untuk mendapatkan perubahan tekanan yang lebih tepat.

TABLE CONTENTS

		Page
SUPERVISOR’S DECLARATION		i
STUDENT’S DECLARATION		ii
ACKNOWLEDGEMENTS		v
ABSTRACT		vi
ABSTRAK		vii
TABLE OF CONTENTS		viii
LIST OF TABLES		xi
LIST OF FIGURES		xii
LIST OF SYMBOLS		xiv
LIST OF ABBREVIATIONS		xv
CHAPTER 1	INTRODUCTION	
1.1	Background	1
1.2	Problem Statement	2
1.3	Project Objectives	2
1.4	Scopes	3
CHAPTER 2	LITERATURE REVIEW	
2.1	The Sun and Solar Position	4
	2.1.1 The Sun Earth Relationship	4
2.2	Solar Collector	7
	2.2.1 Flat Plat Collectors	7
	2.2.2 Evacuated Tube Collector	8
	2.2.3 Flows Through ETSC Panel (SEIDO 2-16)	10
	2.2.4 The Evacuated Tube Solar Collector Efficiency	11
2.3	Fundamentals Of Nanofluids	12

2.4	Nanofluid As Heat Transfer Enhancement	13
2.5	Pressure Drop In The Solar Collector System	17
	2.5.1 Effect Of Nanofluid On The Pressure Drop	18
	2.5.2 Relationship Heat Transfer And Pressure Drop	18
CHAPTER 3	METHADODOLOGY	
3.1	Introduction	21
3.2	Flow Chart	22
3.3	Laboratory Testing Result	23
3.4	Equipment Specification	25
	3.4.1 Manometer	26
	3.4.2 (SEIDO 2-16)	27
3.5	Experimental Setup	27
3.6	Preparation Of Nanofluid	29
	3.6.1 The Step for Preparing Nanofluids	31
	3.6.2 The Step for Dilution Process	33
3.7	Equipment for Preparing Nanofluid	32
CHAPTER 4	RESULT AND DISCUSSION	
4.1	Data Collection	39
4.2	Performance Analysis of Pressure Drop For Distilled Water	39
	4.2.1 Sample Calculation Of Pressure Drop	39
	4.2.2 Performance Analysis at Different Flow Rate	41
	4.2.3 Performance Analysis at Different Temperature	43
4.3	Performance Analysis of Pressure Drop For Nanofluid	49
4.4	Performance Analysis of Difference of Pressure Drop	52

Between Distilled Water and Nanofluid

4.5	Solar Collector Efficiency Performance Analysis	54
	4.5.1 Efficiency of ETSC without Nanofluid	54
	4.5.2 Efficiency of ETSC with Nanofluid	57
CHAPTER 5	CONCLUSION AND RECOMMENDATION	
5.1	Conclusion	59
5.2	Recommendation	60
REFERENCES		61

LIST OF TABLES

Table No.	Title	Page
3.1	U Tube Manometer Specification	25
3.2	Physical properties of nano materials	30
3.3	Specifications of Magnetic Hotplate Stirrer	33
3.4	Specifications of Ultrasonic Homogenizer	35
3.5	Specification of Digital Overhead Stirrer	37
3.6	Specification of KD2Pro	38
4.1	Density of distilled water at different temperature	40
4.2	Specific Heat Capacity at Different Temperature	55
4.3	Relationship Between Pressure Drop and Time with Solar Collector Efficiency for Distilled Water	56
4.4	Relationship Between Pressure Drop and Time with Solar Collector Efficiency for SiO ₂ Nanofluid	58

LIST OF FIGURES

Figure No.	Title	Page
2.1	The Earth's axis is tipped over about 23.5° from vertical	5
2.2	Variation of declination angle δ	6
2.3	Orbit of the earth around the sun	7
2.4	Direct Flow Evacuated tube collector	8
2.5	Heat Pipe Evacuated Tube Collector	10
2.6	Flow of the cold and hot liquid inside the SEIDO 2	11
3.1	Fluid friction apparatus	23
3.2	Graph mass flow rate vs pressure drop	24
3.3	U-Tube manometer	25
3.4	Technical data and specification of SEIDO 2	26
3.5	Schematic diagram of solar collector system	27
3.6	Pressure drop system	27
3.7	The schematic diagram of the experimental system	28
3.8	Nanofluids with high concentration by weight percent	31
3.9	Low concentration of nanofluids by volume percent	32
3.10	Magnetic Hotplate Stirrer	32
3.11	Ultrasonic Homogenizer	34
3.12	Digital Overhead Stirrer	36
3.13	KD2Pro	37
4.1	Flow Rate against Pressure Drop	41

4.2	Time against Temperature and Pressure Drop	43
4.3	Time against Solar Radiation	43
4.4	Time against Temperature and Pressure Drop	45
4.5	Time against Temperature and Pressure Drop	45
4.6	Time against Temperature and Pressure Drop	46
4.7	Pressure Drop against Time	47
4.8	Flow rate vs Pressure drop for nanofluid	49
4.9	Pressure Drop against Time for nanofluid	50
4.10	Time Versus Solar Radiation for nanofluid	51
4.11	Flow rate vs Pressure drop for distilled water and nanofluid	52
4.12	Fouling Effect	54

LIST OF SYMBOLS

W	Mass flow rate
L	Length of Duct
A	Area
g_c	Constant
ρ	Fluid Density
D	Diameter of Duct
f	Friction Factor
v	Velocity
μ	Viscosity
T_o	Outlet Temperature
T_i	Inlet Temperature
T_a	Ambient Temperature
c_p	Specific Heat

LIST OF ABBREVIATIONS

Al_2O_3	Aluminium Oxide
CPC	Compound Parabolic Collectors
CUO	Copper Oxide
ETSC	Evacuated Tube Solar Collectors
FPC	Flat Plate Collectors
SiO_2	Silicon Oxide
TiO_2	Titanium Oxide

CHAPTER 1

INTRODUCTION

1.1 BACKGROUND

Solar thermal systems is a system that use energy from the sun to heat water. This replaces other energy sources such as natural gas and electricity as a means of providing hot water to buildings. Malaysia has an equatorial climate, which has good sunshine, warm and wet weather throughout the year. The demand of hot water and cooling increase by every year and solar system is an alternative way to meet the demand in buildings in an energy efficient way. The solar thermal technologies are used to collect the energy of the sun to provide thermal energy for solar water heating, solar pool heating , solar space heating and cooling, and industrial process pre heating.

The most important part of a solar thermal system is the collector. The collector's role is to absorb the sun's energy and efficiently convert it to heat for transfer to the hot water system. Evacuated tube and flat plate collectors is common main types of thermal solar collectors. Evacuated tube solar collector is better than flat plat collector and ETSC is a system that rapidly becoming the preferred option over flat plate systems in order to get better efficiency.

Pressure drop in a solar collector system is usually a result of resistance caused by friction or other forces acting on a fluid. Pressure drop is one of the factor that can give effect to the efficiency in the whole system and pressure drop system which is can also effect the system performance. The common factor that give effect to pressure drop system are length of pipe , diameter of the pipe, flow of water and roughness of the

inside of the pipe. The higher flow rate and rougher pipe interior surface will give greater pressure drop.

1.2 PROBLEM STATEMENT

Solar system installed in UMP does not measure the pressure drop. Since solar system in UMP does not measure the pressure drop so we don't know the pressure drop in solar collector system at various working fluid and mass flow rate. Temperature mass flow rate and type of working fluid influence the pressure drop it is because according to the literature review in the book *Solar Engineering of Thermal Process* (Foster .R et al,2010) mass flow rate has relationship with pressure drop. The raise of the pressure drop in the solar collector system increase the power consumed to the pump. These situations lead to the decrease of the efficiency of the system. Unstable pressure drop in the solar collector system also is one of the factor that cause solar air collector often have low heat transfer coefficient.

1.3 PROJECT OBJECTIVE

- a) Set up the pressure drop system for solar collector.
- b) Investigate the effect of temperature on the pressure drop
- c) Investigate the effect of nanofluid as working fluid on the pressure drop across the solar collector

1.3 SCOPES

The scopes were:

- 1 Comparison between water and nanofluid pressure drop as working fluid in solar collector
- 2 Evaluate the pressure drop in solar collector at different flow rate and working fluid.

CHAPTER 2

LITERATURE REVIEW

2.1 THE SUN AND SOLAR POSITION

2.1.1 The Sun Earth Relationship

Sun is a sphere with a diameter of 1.39×10^9 consisting of intensely hot gaseous and 1.495×10^{11} m away from the earth. As cited in The Performance of Three Different Solar Panels for Solar Electricity Applying Solar Tracking Device under the Malaysian Climate Condition (Azhar Ghazali et al, 2012), sunlight are available for more than ten hours per day and the irradiation of direct sunlight is between 800W/m² and 1000W/m² with approximate six hour. The weather condition on Malaysia is very suitable to implement solar energy as the alternative energy to replace the existing fossil fuel energy since Malaysia is a Tropicana country which tropical region between 1° N and 7° N, and 100° E and 119° E. (Azhari A.W et al ,2008)

The Earth is rotating around an axis called its rotational axis which is an imaginary line passing through the North and South Poles. The earth is a sphere flattened at the poles and bulging in the plane normal to the poles, which is an oblate spheroid shape. The Earth rotates once in 24 hours and takes 1600 kilometers per hour to rotates at its own axis. The time it takes for the Earth to rotate completely around once is what we call a day and time it takes for the Earth to go around the Sun one full time is what we call a year. The earth rotation that gives us night and day.(John A. D. et al,pg 3-5,2006)

The earth revolves in an elliptic orbit round the sun, with sun at one of the foci of the ellipse. The axis of the earth is tipped over about 23.5° from vertical. As Earth revolves around the sun, the orientation produces a varying solar declination. Declination (δ) is the angle subtended by a line joining the centers of the earth and the sun with its projection on the earth's equatorial plane. .(Foster R. et al, pg 10-15,2010)



Figure 2.1 : The Earth's axis is tipped over about 23.5° from vertical

Source: Monash Science Centre (2006)

Winter season happen when the northern hemisphere tip away from sun meanwhile the summer season when the northern hemisphere tip toward the sun. The declination angle for an nth day may be calculated from the following simple relationship given by Cooper (1969).

$$\delta \text{ (in degrees)} = 23.45^\circ \sin\left[\frac{284+n}{365} * 360^\circ\right]$$

Where n is the total number of days counted from first January till the date of calculation. The figure below shows that the declination angle δ is a sine graph. The zero declination angles δ on March 22(fall) and September 22(spring). Besides that, the minimum declination angle δ change from value -23.5° December 22 to $+23.5^\circ$ on Jun 22.

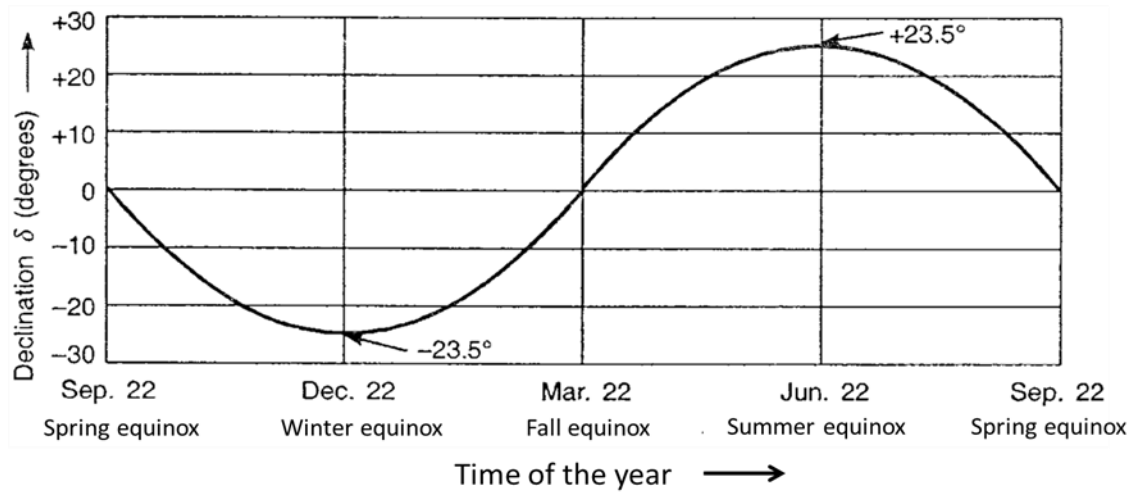


Figure 2.2: Variation of declination angle δ with the nth day of the year

Source: Cooper (1969)

Variations of declination angle affect the optimum tilt angle of solar panel toward the sunlight. During winter season, the solar panel should be mounted at a greater tilt angle in order to get the maximum irradiation of sunlight. Furthermore, the tilt angle of solar panel should be mounted at a smaller angle to achieve the optimum performance. For spring and fall season, the declination angle is zero, in order to maximum the energy production, the solar panel should mount at an angle between winter and summer seasons (Robert Foster, pg 7-9,2010).



Figure 2.3 : Orbit of the earth around the sun

Source: Tiwari, (2004)

2.2 SOLAR COLLECTOR

In the solar system solar collector is the major component and a special kind of heat exchangers that transform solar radiation energy to internal energy of the transport medium.

There are three types of stationary solar collector, which are Flat Plate Collectors (FPC), Stationary Compound Parabolic Collectors (CPC) and Evacuated Tube Collectors (ETC). Although there are great geometric differences, their purpose remains the same which is to convert the solar radiation into heat to satisfy some energy needs.

2.2.1 Flat Plat Collectors

A flat plat solar collector consists of a waterproof, metal or fiberglass insulated box containing a dark coloured absorber plat , the energy receiver, with one or more translucent. Absorber plate are typically made out of metal due to its high thermal conductivity and painted with special selective surface coatings in order to absorb and transfer heat better than regular black paint can. The glass cover help reduce the

convection and radiation heat losses to environment. Most of the heat loss through the top section and that will decrease its efficiency.(Foster R.et al,2010)

2.2.2 Evacuated Tube Collector

The evacuated tube solar collectors perform better and more efficient compared to flat plate solar collectors, in particular for high temperature operations . ETSC was in the market for over 35 years. It can achieve higher temperature but it is more expensive compared to the FPC. The evacuated solar collector are useful for commercial and industrial heating applications and its is an alternative to flat plat collector especially in areas where it is often cloudy where flat plat collector can only be used under warm area and the at the time when the intensity of the solar radiation is substantially high. Evacuated tube solar collector is not sensitive of climate change.(Soteris A. K. ,2004).



Figure 2.4 : Direct Flow Evacuated tube collector

Source: Kratzenberg, (2006)

An evacuated-tube collector contains several rows of glass tubes connected to a header pipe. Each tube has the air removed from it (evacuated) to eliminate heat loss through convection and radiation. Inside the glass tube, a flat or curved aluminum or copper fin is attached to a metal pipe. The fin is covered with a selective coating that transfers heat to the fluid that is circulating through the pipe. ETSC also consists of two glass tube which made of extremely strong glass. The outer tube has very high transitivity and low reflectivity which enable the radiation to pass through. The inner tube has a selective coating layer which can maximizes absorption of solar energy while minimizes the refection, thereby it locking the heat. The tubes which are sealed with copper pipe continuously bonded to a selectively coated copper fin or absorber plate which collects the solar energy and convert it to heat. Further, the tubes are evacuated and have a barium getter (vacuum indicator) which changes color from silver to white if a tube's vacuum has been compromised. Generally there are two main types of evacuated tube collectors (Robert Foster, 2010).

Direct Flow Evacuated Tube Collector

A direct flow evacuated tube collector in figure 2.4 has two pipes that can run inside the tube. One of the pipes is for the inlet fluid and the other one for the outer fluid. The pipes enable the working fluid to flow in and out of the inner. All the pipes are fitted to the header separated the inlet from the inlet. (Foster R.et al,2010)

Heat Pipe Evacuated Tube Collector

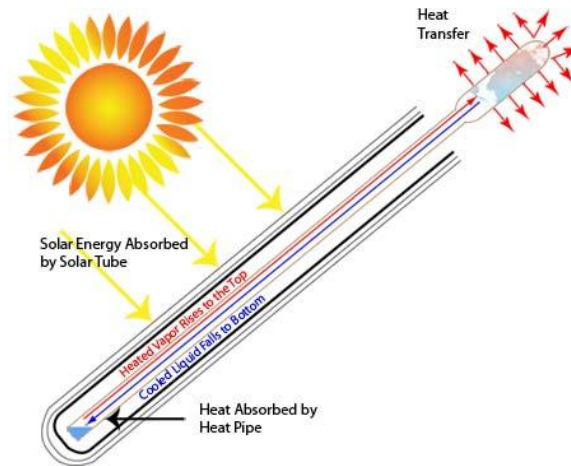


Figure 2.5: Heat Pipe Evacuated Tube Collector

Source : Morrison (2004)

In a heat pipe evacuated tube collector in Figure 2.5, each vacuum sealed glass tube allocates one metal pipe usually copper, attached to an absorber plate. The purpose of the vacuum is to easily change from the liquid phase to a vapor because water boils at a lower temperature when pressure is decreased. Vaporization is achieved around 25-30 ° C, so when the heat pipe is heated above this, vapor rapidly rises to the top of the heat pipe, transferring heat. As the heat is lost, the vapor condenses and returns to the bottom for the process to be repeated. (Foster R. et al, 2010)

2.2.3 Flows Through Evacuated Tube Solar Collector Panel (SEIDO 2-16)

SEIDO 2 is direct flow evacuated tube. Configuration and appearance are similar to SEIDO 1 but the heat pipe is replaced by a coaxial set of copper tubes. The heat transfer from the absorber to the heat circulation is performed by applying flow through. The evacuated tube collector is sealed with thermo-compression sealing technology to prevent heat losses. Moreover, this panel provides protection from corrosion. The

aluminium nitride selective coating on the absorber plate ensures the exceptionally high solar absorption and low thermal emission of the tubes.

Customisation and Convenience

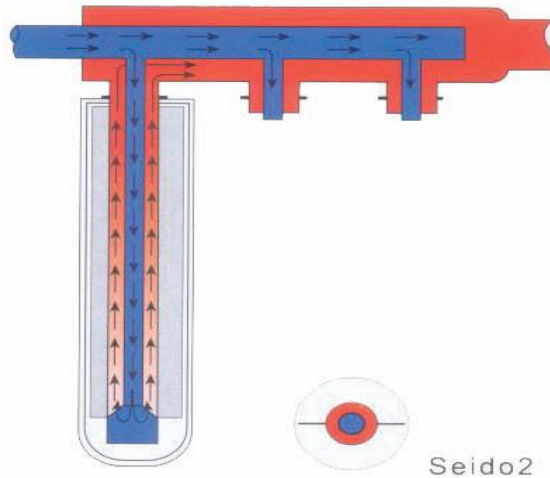


Figure 2.6: Flow of the cold and hot liquid inside the SEIDO 2

Source: Morrison (2004)

SEIDO 2 solar collector applies a flow through design which increases their efficiency. The heat transfer liquid flows through a concentric tube integrated into the absorber picking up thermal energy by direct heat exchange. The cold liquid is inducted through the inner tube. It flows back in the gap between the inner and outer tube. The inlet and outlet tube of each collector tube are connected to the manifold. All tubes are connected in parallel.

2.2.4 The Evacuated Tube Solar Collector Efficiency

The instantaneous efficiency for the evacuated tube were calculated using the following correlation.

$$\eta = [\dot{m}C_p(T_{out} - T_{in})]/A_c G_T \quad (2.1)$$

Where G_T is the gross area which refers to the external mass of the collector or the area actually necessary for installation, that is simply the length times the width of the

collector and A_C is aperture area which is the area through which solar energy enters the collector.

Or

$$\eta = \eta_0 - a \frac{(T_m - T_a)}{G} - b \left[\frac{T_m - T_a}{G} \right]^2 \quad (2.2)$$

in which the correlation coefficient η_0 , constant a , and constant b are to be evaluated either analytically or experimentally.

The overall efficiency of water-in-glass tubes was described by the correlation,

$$\eta = 0.58 - 0.9271 \frac{(T_m - T_a)}{G} - 0.0067 \left[\frac{T_m - T_a}{G} \right]^2 \quad (2.3)$$

The overall efficiency of heat-pipe was described by the correlation,

$$\eta = 0.8097 - 1.7828 \frac{(T_m - T_a)}{G} + 0.0119 \left[\frac{T_m - T_a}{G} \right]^2 \quad (2.4)$$

2.3 FUNDAMENTALS OF NANOFLUIDS

Stable and highly conductive nanofluids are produced by one and two step production method and both of this method is approaches to avoid nanoparticle suspension from agglomerate.

In two step method nanoparticles must be synthesized first before disperses them into base fluids. The one step method simultaneously makes and disperses nanoparticles directly into base fluid. Well mixed nanoparticles is needed to get a good product of nanofluids.

Nanoparticles produced in the dry powder form will form some agglomeration occur due to strong attractive van der Waals forces between nanoparticles. Well dispersed stable nanoparticle suspensions are produced by fully separating the agglomerates nanoparticles into individual nanoparticles in the liquid and we cannot get the good products of nanofluids produced by two step method because the individual particles in the liquid will quickly agglomerate before dispersion hence will produced poor dispersion quality. Conductivity of the nanofluids is low if the dispersion quality is poor therefore nonagglomerated nanoparticles in the liquids must be produced in order

to achieve significant enhancement in the thermal properties of nanofluids (Das, S. K et al, 2008).

Des et al ,2003 discovered that nanofluids conductivity have a strong relationship with a temperature. It shown that water based nanofluids containing Al_2O_3 nanoparticles increase in thermal conductivity enhancement over a small range of temperature which is within 20 and 50 °C . The good relationship between temperature and thermal conductivity is due to motion of nanoparticles.

The fact that the thermal conductivity of the suspensions is higher than that of the base fluid is nothing new. Model for thermal conductivity of suspensions which is clearly indicated the higher value of thermal conductivity has been proposed by Maxwell ,1881. This is primarily due to the fact that the solids have orders of magnitude higher thermal conductivity than that of liquids. The liquids have poor thermal conductivity for example water has thermal conductivity of 0.6 W/m.k which is lower than that of solid oxides.

However, although these higher conductivities are attractive from the view point of cooling capabilities, other problems associated with suspensions, such as sedimentation, clogging, fouling, erosion, and excessive pressure drop, make them unsuitable for cooling applications.

2.4 NANOFLUID AS HEAT TRANSFER ENHANCEMENT

A nanofluid is a liquid mixture with a small concentration of nanometer sized solid particles in suspension and these combination of nanoparticles and liquid have been shown to substantially increase the thermal conductivity of the nanofluid over the base liquid. Nanofluid are found to exhibit higher thermal conductivity even at very low concentration of suspended nanoparticles.(Wenhua Yu ,2009)

Poor thermal conductivity of working fluid had limit the heat transfer performance so dispersing the micrometer sized particle in liquids has be done in order

to improve the heat transfer performance. Heat transfer is one of the most important process in many industrial and consumer products (Das, S. K et al,2008) .

Nanofluids are relatively new class of fluids which consists of a base fluid with nano sized particles less than 100 nm suspended within them. As cited in A combined model for the effective thermal conductivity of nanofluids (Murshed S.M.S et al,2009) nanofluids provide higher thermal conductivity compared to basefluids and its value increase with particles concentration, temperature, particles size, dispersion and stability. Stability of nanofluids have good corresponding relationship with the enhancement of thermal conductivity where the better dispersion behavior, the higher thermal conductivity of nanofluids. The dispersion of the nanoparticles could be influenced by time. It was found that fresh nanofluids exhibited slightly higher thermal conductivities than nanofluids that were stored up to two months due to reduced dispersion stability of nanoparticles with respect to time which is nanoparticles may tend to agglomerate when kept for long period of time.

Nanofluids as fluids have fewer problem relative to suspensions with larger particles such as sedimentation, erosion, additional pressure drop and non- Newtonian behavior in low concentrations. Relative heat conductivity are much more when the concentrations of the nanoparticles are greater than when the concentrations are lower, which is thought to be due to the increase in the nanolayer thickness and Brownian motion of the equivalent particle. As the nanolayer thickness is increased the relative heat conductivity is astonishingly increased. Rate of this increase with temperature is independent of nanolayer thickness and nanolayer heat conductivity. This is thought to be due to independence of the nanolayer formation from temperature. As the nanolayer thickness is increased, the heat conductivity is increased. This is thought to be due to an increase in the Brownian motion of the particles. It has to be pointed out that the Brownian motion of the particle is decreased as the size of the particle is increased, suggesting that the nanolayer to have a different effect on the heat conductivity of the Nanofluids compared with the size of the particles (Izadi, M. et al,2009).

Excellent characteristics of nanofluids such as enhanced thermal conductivity, long time stability and little penalty in pressure drop increasing and tube wall abrasion have motivated many researchers to study on thermal and flow behavior of nanofluids.

When nanoparticles are properly dispersed, nanofluids can offer numerous benefits besides the anomalously high effective thermal conductivity. Some of these benefits are improved heat transfer and stability, microchannel cooling without clogging, miniaturized systems, and reduction in pumping power. The better stability of nanofluids will prevent rapid settling and reduce clogging in the walls of heat transfer devices. The high thermal conductivity of nanofluids translates into higher energy efficiency, better performance and lower operating costs.

In addition to the Brownian motion of nanoparticles, this model also takes into account several other key factors such as particle size, fluid temperature and interfacial nanolayer that also contribute to the enhancement of the effective thermal conductivity of nanofluids. The conventional kinetic theory-based Brownian motion term has been renovated using effective diffusion coefficient concept (Sohel Murshed S. M., 2011)

A wide range of experimental and theoretical studies has been performed on the effect of different parameters such as particle concentration, particle size, mixture temperature and Brownian motion on thermal conductivity of nanofluids. The results showed an increase in thermal conductivity of nanofluid with the increase of nanoparticles concentration and mixture temperature (Pirhayati, M ,2012).

Another property that influenced the thermal conductivity is the density and viscosity which is will increase pressure drop and pumping power. The viscosity of nanoparticles water suspensions increase with increasing particle concentration in the suspension (Saidur R. et al ,2011).

Through the experiment designed in Nanofluids in a Forced-Convection Liquid Cooling System to measure the convective heat and pressure through cold plate it has been conclude that the heat transfer coefficient increased with the increased of pumping

power. The experiment used CUO and AL₂O₃ to water in volume to form the nanofluids. The higher the concentrating of the mixture by volume will also increase the pumping power at fixed heat transfer coefficient. The operating cost related to pumping power due to increase viscosity of the fluid also need to be considered in the design and selection (Kaltah M. et al ,2012).

Higher thermal conductivity of nanoparticles is one of the reasons for better heat transfer performance of nanofluids. The Nusselt number contains both effects of thermal conductivity and heat transfer coefficient and is a criteria for heat transfer performance of any fluid. However, nanofluid's thermal conductivity enhancement is noticeable only when the nanoparticle concentration is higher than 1 vol.%. Therefore, higher Nusselt number for nanofluid with lownanoparticle concentration is due to the heat transfer coefficient enhancement (Buongiorno et al,2009).

Particle dispersion in liquids can give higher thermal conductivity. Al₂O₃ nanoparticles when dispersed in water can significantly enhance the convective heat transfer in the laminar flow regime and the enhancement increases with Reynolds number, as well as particle concentration compared to base fluid. Nanofluid give higher heat transfer rates compared to base fluid water and the value increases with increase in volume concentration. This is due to higher values of nanofluid thermal conductivity (material ability to conduct heat). The heat transfer enhancement at 0.5% volume concentration and at Reynold number of 22,000 shows 15.99 % higher compared to water (Sharma K .V et al 2010) .

Experimental result of the convective heat transfer also showed that Al₂O₃/water CuO/water showed Al₂O₃/water have higher heat transfer enhancement compared to cooper oxide CuO (Heris et al,2006). Heat transfer coefficient and Nusselt number increase with the Reynold number and volume concentration.

Two different concentration of Al₂O₃/water 1.5 and 3% wt was prepared to shows the influence of the nanoparticle concentration on the temperature difference and

it can be seen that by increasing the nanofluid concentration the temperature difference will decreased (Moraveji M.K.et al ,2012).

One of the most effective properties of a fluid in heat transfer is its thermal conductivity Practically, using large sized particles is unfeasible, since they cause some problems such as sedimentation of particles, erosion, and pressure depreciation which make the fluid's movement impossible. Nanofluid has some advantages such as large specific surface area, high thermal conductivity, low erosion and proper stability. Generally, there is a remarkable difference between thermal conductivity of nanoparticles used in preparing nanofluid and thermal conductivity of the base fluids. For this reason, adding nanoparticles to a base fluid is expected to make reasonable changes in the fluid's thermal conductivity (Nasiri M. et al,2011).

2.5 PRESSURE DROP IN THE SOLAR COLLECTOR SYSTEM

In many systems pressure drop is most often expressed as the equivalent fluid head loss h in terms of meters or feet of water, a convenient fluid for measurement of the pressure drop. The water pressure in a system is not only depend on water column height, but also on the friction from the movement of water in a pipe, as well as any drop in the static water level due to pumping. (John A. D ,William A. B ,pg 166-171, 2006).

Pressure drop is a term used to describe the differential pressure that a fluid must overcome to flow through a system. Pressure drop is a result of resistance caused by friction or other forces acting on a fluid. Any type of obstruction, restriction or roughness in the system will cause resistance to air flow and cause pressure drop. In the distribution system, the highest pressure drops usually are found at the points of use, including in undersized leaking hoses.

Pressure drop is one of the factor that can give effect to the efficiency in the system where excessive pressure drop will lead to poor results in system performance and excessive energy consumption and this will lead to decreased of efficiency of the

system. Energy needed for pumping yet maintaining flow rate should be minimize to allow system to operated efficiently in the pressure drop system.(Steve P. S,2010)

2.5.1 Effect Of Nanofluid As Working Fluid On The Pressure Drop

By passing laminar nanofluid flow in heated tube, it has been found that using the nanofluid increase the bouyancy of secondary induced flow and decrease friction at the inner wall. The effects of adding nano diamond with different concentration to engine oil on the pressure drop inside the microfin tube under constant heat flux at the outer wall and laminar nanofluid flow conditions was investigated by Akhavan-behabadi et al, 2010. The results show an increase in pressure drop with enhances nano particle concentration.

Adding additives into nanofluid in order to remove heat from high heat flux surfaces also have shown anti wear and anti-friction characteristics result in reducing pressure drop (Battez, A.H. et al, 2008).

Pressure drop has been measured along the round tube with different weight fractions of nanofluids and the results show that, with increase nanoparticle concentration, the pressure drop increase in both horizontal and inclined tube. The obtained results show that the tube inclination have decreased pressure drop remarkably compared to that of horizontal tube at low Reynolds number. This can also lead to wall shear stress decreasing which results in pressure drop decline (PirhayatI M.,2012). Besides that increase the thermal conductivity is larger than the increment in pressure drop due to increase in viscosity for all range of selected volume fractions.

2.5.2 Relationship Between Heat Transfer Coefficient And Pressure Drop

In the pressure drop system it necessary to take note about length of pipe , diameter of the pipe, flow of water and roughness of the inside of the pipe it is because all of this will give effect to the pressure drop where longer and smaller pipe will give greater pressure drop. Higher flow rate and rougher pipe interior surface also contribute

to greater pressure drop. The length of the pipe and speed of water also can cause an increased to the pressure drop and higher pumping power requirement. (Foster R. et al, pg 208-213 ,2010)

An important fundamental relationship for the duct fluid that runs in the collector is the Fanning equation as expressed in the Eq (2.5) (Elradi A. M. et al, 2004)

$$\Delta P = \frac{4fW^2L}{2g_c A^2 \rho D} \quad (2.5)$$

The friction factor is given by:

$$f = 16/Re \quad (2.6)$$

and the Reynold number is given by

$$Re = \frac{\rho v D}{\mu} \quad (2.7)$$

Based on the equation reynold number shows in Eq (2.7) above, for high reynold number, pressure drop over the collector is direct proportional to the change in the density for the constant velocity. The variation in reynold number also dependent on kinematic viscosity μ .(Albanakis C. et al, 2009) .

The determination of the heat transfer coefficient, h, in the solar collector system is:

$$h = mc_p \frac{(T_o - T_i)}{A(T_m - T_a)} \quad (2.8)$$

Based on the experiment of effect of the solar radiation on the thermal efficiency on the double-pass solar collector it can be conclude that with higher porosity, the increased mass flow rate through this area increased the heat transfer coefficient. Efficiency also will increases as temperature rise increases. Pressure drop in the collector increases depends on the heat transfer area and temperature rise. The pressure drop through the collector depends on the losses such as at the upward edges, the sides and the back. In the double-pass solar collector, the mass flow rate has more effect on the temperature rise. Pressure drop and flow rate are dependant on one another. The higher the flow rate through a restriction, the greater the pressure drop. Conversely, the

lower the flow rate, the lower the pressure drop. With the increase in flow rate the velocity of the fluid increases. and with the increase in velocity the pressure decreases, because there will be pressure drop. The solar radiation has more effect on temperature rises at low porosity. In addition, the Reynolds number has more effect than the Nusselt number at low porosity. Heat transfer coefficient increases by using more porous media in the lower channel of the double-pass solar collector. (Elradi A. M et al, 2004)

In all cases the increase of the average surface temperature resulted in increased values of pressure drop. Concerning the air temperature at the outlet, decreased of the inlet velocity, will give better heat exchange between inlet air flow and the specimen, due to increased in the available time for the heat transfer and thus to a higher outlet air temperature. (Albanakis C. et al, 2009) .

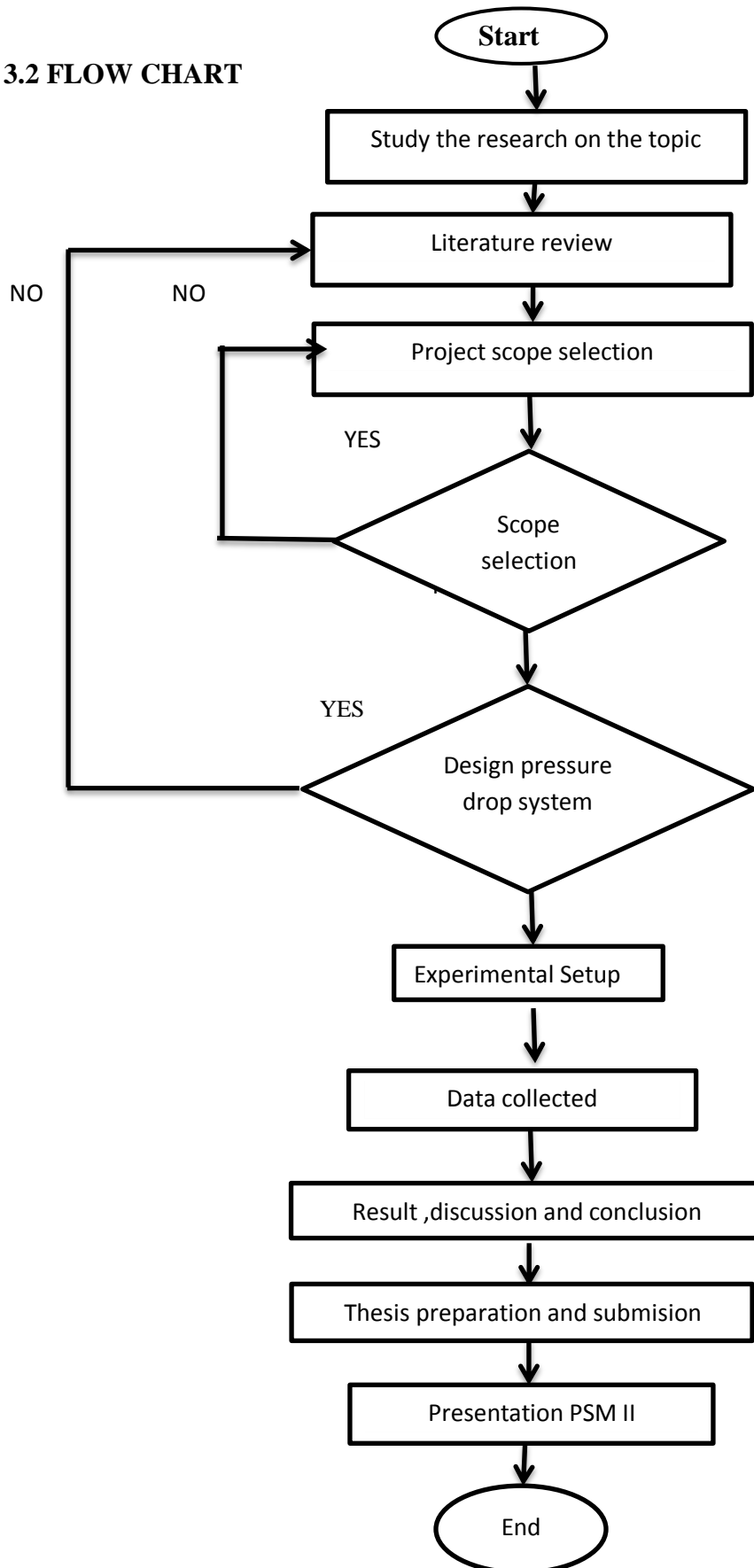
CHAPTER 3

METHODOLOGY

3.1 INTRODUCTION

A systematic planning is important before doing any research. In methodology all the procedures and method use to study the pressure drop is shown.

3.2 FLOW CHART



3.3 LABORATORY TESTING RESULT



Figure 3.1: Fluid friction apparatus

The preliminary testing for pressure drop was carried out by fluid friction apparatus like shown in the Figure 3.1. The testing were carried out by using 800 mm PVC straight pipe section and 90° bend pipe with mass flow rate from 0.9 to 3.6 l/min. All the result obtained from the testing were showed in the Figure 3.2.

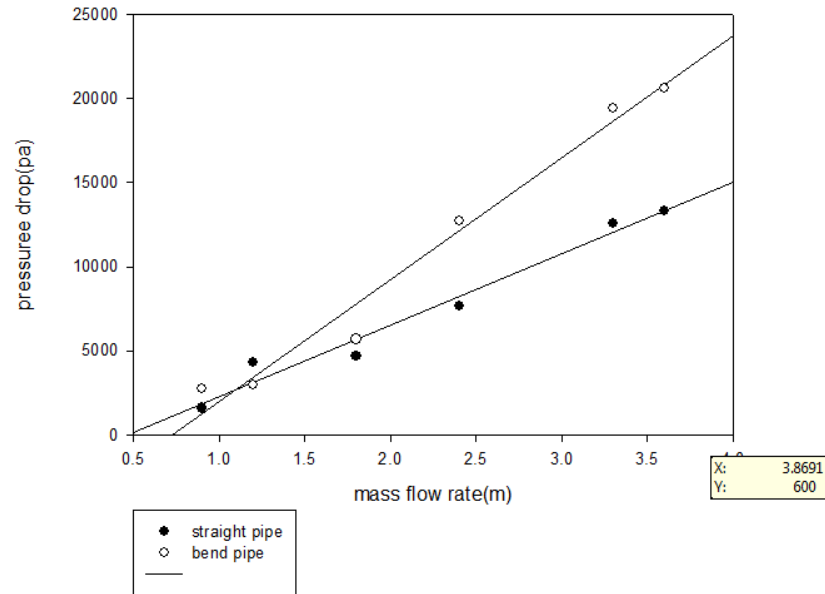


Figure 3.2: Graph mass flow rate vs pressure drop

Based on the Figure 3.2 the result shows that bend pipe give higher pressure drop compare to the straight pipe. The graph above shows that pressure drop is directly proportional to mass flow rate where the pressure drop increased when the mass flow rate increased.

Based on the Figure 3.2, for the bend pipe the minimum pressure drop is 2452.5 pa which is at 0.9 l/min and the maximum pressure drop is 20,601 pa at 3.6 l/min. For the straight pipe the minimum pressure drop is 1569.6 pa and maximum pressure drop is 13341.6 pa.

3.4 EQUIPMENT SPECIFICATION

3.4.1 Manometer

U-Tube manometer is an instrument for the measurement of pressure. U-shaped glass tube partially filled with water, one side of which is connected to the source of pressure. The amount of displacement of the liquid (height of the column of the distilled water) is a measure of the magnitude of the pressure.



Figure 3.3: U-Tube manometer

Table 3.1: U Tube Manometer Specification

Model	RM 1001
Brand	Lanxi of China
Technical Specification	U" Tube type Primary standard Manometer used for precision measurement of pressure, vacuum, differential pressure, and flow measurement
Range	0-50mbar

3.4.2 (SEIDO 2-16)

SEIDO 2 solar collector applies a flow through design which increases their efficiency. The heat transfer liquid flows through a concentric tube integrated into the absorber picking up thermal energy by direct heat exchange. The cold liquid is inducted through the inner tube. It flows back in the gap between the inner and outer tube. The inlet and outlet tube of each collector tube are connected to the manifold. All tubes are connected in parallel. This are shown in the Figure 2.6.

SEIDO 2 solar collectors collect heat from sun working in high efficiency and absorbing up to 92% of the incoming irradiation. With the excellent efficiency, SEIDO 2 solar collectors can be applied in domestic water heating for household and even larger systems for commercial or public use, space heating and air conditioning.

Module type	SEIDO2-8		SEIDO2-16	
Tube construction	SEIDO2---Direct flow vacuum tube with flat absorber			
Certificate	EN 12975			
Angle of inclination	0° to 90°			
Number of collector tubes	8		16	
Absorber area	1.39 m ²		2.77 m ²	
Aperture area	1.47 m ²		2.93 m ²	
Gross area	2.04 m ²		4.08 m ²	
Length x width x height (mm)	2126x960 x150		2126x1920x150	
Weight	50 kg		100 kg	
Pressure drop per module	<7 mbar (100L/h)	<20 mbar (200L/h)	<7 mbar (100L/h)	<20 mbar (200L/h)
Fluid content per module	1.3 L	2.6 L	1.3 L	2.6 L
Glass material	Borosilicate glass			
Glass tube diameter	100			
Wall thickness	2.5 mm			
Transmittance	> 0.90			
High vacuum, long term stability	< 10 - 5 mbar			
Absorber material	Aluminum			
Selective coating	Aluminum nitride			
Absorptance	> 0.92			
Emittance	< 0.08			
Header box material	Aluminum			
Header box size	958x108x126mm	1918x108x126mm	958x108x126mm	1918x108x126mm
Insulation	Polyurethane foam			
Max. operating pressure	6 bar			
Stagnation temperature, module	190°C			
Stagnation temperature, pipe	247 °C			
Assembling components	Stainless steel vertical supports and bottom supports, aluminum header box, 30 mm thickness polyurethane insulation			
Connection	Compression fitting 22 mm			

Figure 3.4: Technical data and specification of SEIDO 2

Source: A. Walker (2004)

3.5 EXPERIMENTAL SETUP

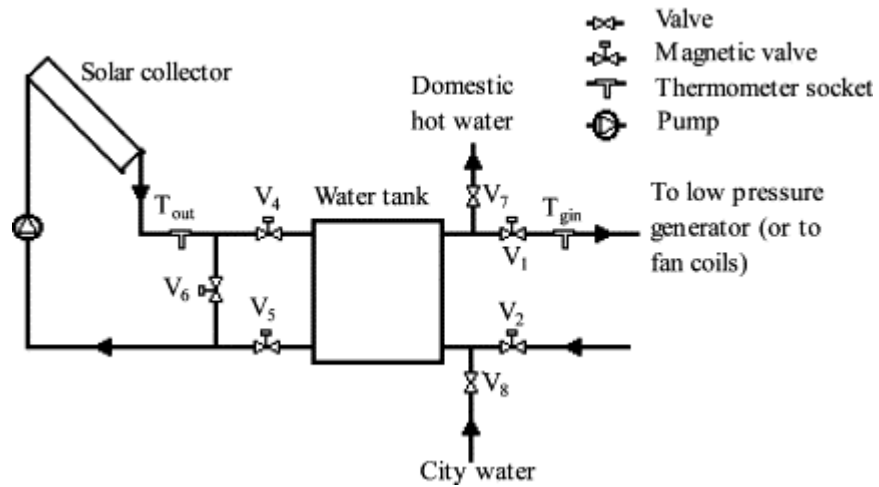


Figure 3.5: Schematic diagram of solar collector system

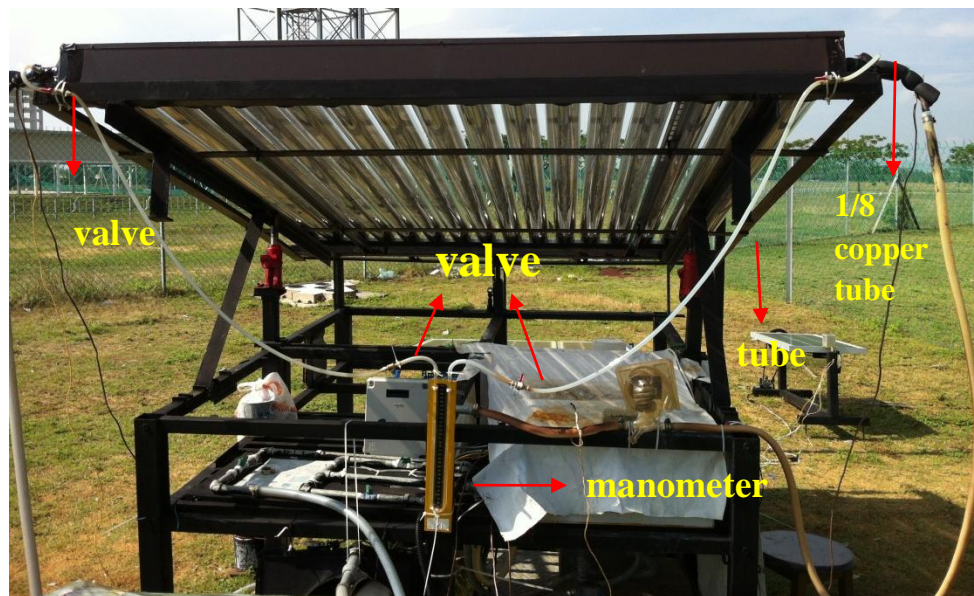


Figure 3.6 : Pressure drop system

Figure 3.5 shows a schematic diagram of a solar collector system which shows how the system operated. Figure 3.6 shows schematic diagram of the pressure drop system. It essentially consist of 1/8 “ copper tube, valve, manometer which is used to

measure height of water column and nylon tube to connect from copper tube to manometer. 1/8 inches of hole is drilled at 1/2 “ copper tube which was fixed with collector to make hole so that can connect the 1/2 “ of copper tube to the 1/8” of copper tube. A valve was also fixed at the system so that can controls the flow and pressure within a system. Pressure drop system shown in the figure 3.6 were schematically shown in the figure 3.7.

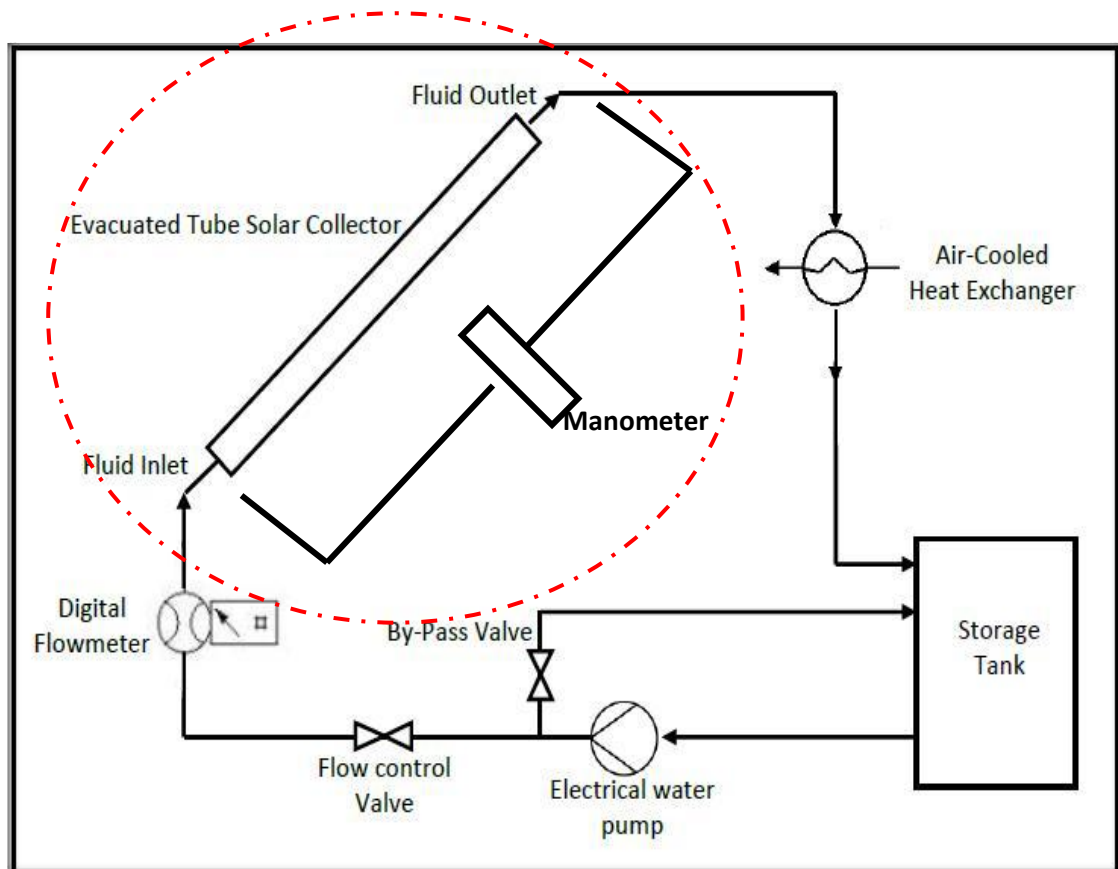


Figure 3.7. The schematic diagram of the experimental system

The data of pressure drop was collect by vary the mass flow rate with different working fluid. The value of inlet , outlet and ambient were recorded.

3.6 PREPARATION OF NANOFLUIDS

3.6.1 The Step for Preparing Nanofluids In Two Step Method

The amount of nanoparticles required for preparation of nanofluids is calculated using the law of mixture formula. A sensitive balance is used to weight the nanoparticles is very accurately. The weight of the nanoparticles required for preparation of 100ml nanoparticle of a particular volume concentration. By using water based fluid is calculated by using the following relation[2],

$$\phi = wt\% = \frac{m_p}{m_p + m_w} \quad (3.1)$$

$$\phi = v\% = \frac{V_p}{V_p + V_m} = \frac{\frac{m_p}{\rho_p}}{\frac{m_p}{\rho_p} + \frac{m_w}{\rho_w}} \quad (3.2)$$

From equation (3.1),

$$m_w = \frac{(1-\phi)m_p}{\phi} \quad (3.3)$$

Substitute equation (3.3) into (3.2),

$$\phi = \frac{\frac{m_p}{\rho_p}}{\frac{m_p}{\rho_p} + \frac{[(1-\phi)m_p]}{\phi\rho_w}}$$

Therefore,

$$\phi = \frac{\rho_w}{\rho_w\phi + (1-\phi)\rho_p} \quad (3.4)$$

Table 3.2 : Physical properties of nano materials

Particle	Investigator and Reference	Particle dia. nm	Thermal Cond. W/mK	Density kg/m ³	Specific heat J/kgK
Al₂O₃	Pak and Cho	13	36*	3880*	773*
	Vajjha and Das	53	36	3600	-
	Williaams et al.	46	-	3920	-
Cu	Chen et al.	50	-	-	554
	Xuan and Li	~100	-	-	-
	Data Book	35	383*	8954*	386*
CuO	Vajjha and Das	29	17.65	6500	-
	Fotukian and Esfahany	30-50	69*	6350*	535.6*
	Mintsa et al.	29	-	6500	-
SiC	Yu et al.	170	-	-	-
	National Ins. Of Standard and Tech.	-	-	3169	725
	Data Book	-	490*	3160*	675*
SiO₂	Vajjha and Das	20-100	1.4	2220*	745*
	Hwang et al.	12	1.38*	2220	-
	Pak and Cho	27	8.4*	4175*	692*
TiO₂	He et al.	21	13.7	4170	-
	Duangthongsuk and Wongwises	27	8.48	-	-
	Vajjha and Das	29 and 77	13	5600*	514*
ZnO	Hong et al.	10-60	29*	-	-
	Williams et al.	60	-	5500	-
	Data Book	-	1.7*	5500*	502*
Fe₃O₄ (magnetite)	Manahan	36	6*	5180*	670*
	Wikipedia Engineeringtoolbox				

*The value used in the present analysis

The density of nanoparticles is taken from the **Table 3.2**.

Then, proceed the preparation step with mix the nanoparticles with water based by using magnetic stirrer. The nanoparticle and water mix for about 10 to 15minutes. After that, immediately put the fluids onto the ultrasonic homogenizer. This is to avoid the fluid to settle down. At the ultrasonic homogenizer, the nanoparticle and water will homogenize and become nanofluid with the calculated concentration. To produce a big volume of nanofluids, the digital overhead stirrer is used.

3.6.2 The Step for Dilution Process

The dilution process consists of simultaneously making and dispersing the particles in the fluid. The dilution process can uniformly dispersed nanofluids and it can be stably suspended in the base fluid. The dilution process is about the high concentration of nanofluids (**Figure 3.8**), will be dilute with magnetic stirrer to low concentration of nanofluids (**Figure 3.9**). By using the previous equation (2) to measure the concentration, we have to do some calculation in equation (5).

$$m_1 \cdot V_1 = m_2 \cdot V_2 \quad (5)$$



Figure 3.8: Nanofluids with high concentration by weight percent



Figure 3.9: Low concentration of nanofluids by volume percent

3.7. EQUIPMENT FOR PREPARING NANOFLUID

3.7.1 Magnetic Hotplate Stirrer



Figure 3.10: Magnetic Hotplate Stirrer

Equipment in Figure 3.10 is for mixing the nanoparticles with water based. It also can use for dilute the high concentration of nanofluids to low concentration of nanofluids. It has small oval of magnetic that will stir the liquid at the bottom of it.

Table 3.3: Specifications of Magnetic Hotplate Stirrer

Model	LMS-1001
Type	Magnetic Stirrer
Speed Range	60 to 1500rpm
Temperature Range	N/A
Controller	Electronic Solid State Controller
Material	Ceramic Coated Stainless Steel Top Plate
Dimension Plate	190 mm × 190 mm
Dimension Overall	205 × 260 × 110 (mm) (W×D×H)
Power Consumption	Max. 800W, 4A
Voltage	110V,60Hz

Source: Murshed (2009)

3.7.2 Ultrasonic Homogenizer



Figure 3.11: Ultrasonic Homogenizer

Equipment in the Figure 3.11 was used to homogenize the nanopowder with the water and to apply ultrasonic treatment to substance using cavitation effect created in the liquid by ultrasonic waves.

Table 3.4: Specifications of Ultrasonic Homogenizer

Working frequency range	21~35kHz, frequency auto-tracking
Time control precision	$\pm 1\%$ can be set freely
Ultrasonic time setting	0.1~9.9s, LCD display
Interval time setting	1~10000s, LCD display
Total ultrasonic time setting	999M, LCD display
Temperature protection range	0~99°C
Ultrasonic power	950W, LCD display (2~99%W)
Duty ratio	0.1~0.99
Working voltage	220V/110VAC $\pm 5\%$, 50/60Hz
Working environment	Indoor (free from moisture, sunlight and corrosive gases)

Source: Murshed (2009)

3.7.3 Digital Overhead Stirrer



Figure 3.12: Digital Overhead Stirrer

This equipment in the Figure 3.12 is to mix and stir the nanofluids with the high volume. This is because to prepare the nanofluids to be used in solar is about 10litres. So, if using the magnetic stirrer is not compatible. This equipment can stir and also use for dilute the high concentration of nanofluid to low concentration. This digital overhead stirrer can control the speed of propeller stirrer and the velocity revolution is appearing in digital that easy to fix and see.

Table 3.5: Specification of Digital Overhead Stirrer

Speed Range	60~2400 min⁻¹
Speed Display	LED display
Measurement fault	Max. $\pm 0.5\%$ ± 30 Digit
Normal Voltage	230 $\pm 10\%$
Frequency	60Hz
Input Power	87W
Power Output	20 + 35%
Overall Efficiency	40%

Source: ika.com, retrieved at 16 October 2012

3.7.4 KD2Pro



Figure 3.13: KD2Pro

Propose: The KD2 Pro in the figure 3.13 is a fully portable field and lab thermal properties analyzer. It uses the transient line heat source method to measure thermal conductivity, resistivity, diffusivity, and heat capacity. To measure the thermal properties of nanofluid, mostly are using this

equipment. It consists of a handheld controller and sensors that can be inserted into the medium you wish to measure. The single-needle sensors measure thermal conductivity and resistivity; while the dual-needle sensor also measures volumetric specific heat capacity and diffusivity.

Table 3.6:Specification of KD2Pro

Operating Environment	Controller : 0~50°C Sensor : -50~+150°C
Power	4AA cells
Battery Life	Approximate 1800 readings in constant use 3years with no use
Case Size	15.5 × 9.5 × 3.5 (cm)
Display	LCD graphics
Keypad	Sealed membrane
Data Storage	4095 measurement in flash memory
Sensor Cable Length	0.8m
Read Modes	Manual and auto read
Sensors	1) single-needle (6cm) 2) single-needle(10cm) 3) dual-needle (30mm)

Source:..Saidur (2011)

CHAPTER 4

RESULT AND DISCUSSION

4.1 DATA COLLECTION

The data for pressure drop were collected by using pressure drop system installed at solar house UMP Pekan. The data were collected by using two different working fluid which is distilled water and nanofluid. The height of a column of distilled water and silicon oxide were measured in order to get the value for pressure drop. The experiment were run by using flow rate start from 2 litre per minute until 3.5 litre per minute by incremental of 0.5 litre per minute. and this experiment was run only on the sunny day. The readings from this experiment were analysis using plotted graph in order to compared the value of pressure drop by different working fluid and flow rate.

4.2 PERFORMANCE ANALYSIS OF PRESSURE DROP FOR DISTILLED WATER SOLAR SYSTEM

4.2.1 Sample Calculation Of Pressure Drop

The pressure drop were calculated by using the pressure drop formula by multiplying the density of distilled water with gravity and height of a column of distilled water. The density of distilled water is difference for different temperature. The pressure drop is calculated by using the density as shown in the table 4.1 below.

Table 4.1 : Density of distilled water at different temperature

TEMPERATURE (°C)	DENSITY (kg/m³)
30	996
40	992
50	988
60	983

Source : C.R. Snelling, (2008)

By using the formula $\Delta P = \rho g h$, the pressure drop were calculated and determine. The value of h were obtained from data collected from the experiment.

Sample Calculation

At flow rate 2 litre per minute

$$\Delta P = \rho g h$$

$$\Delta P = (992 \text{ kg/m}^3) (9.81 \text{ m/s}^2) (0.07 \text{ m})$$

$$= 694 \text{ Pa}$$

4.2.2 Performance Analysis Of Pressure Drop at Different Flow Rate

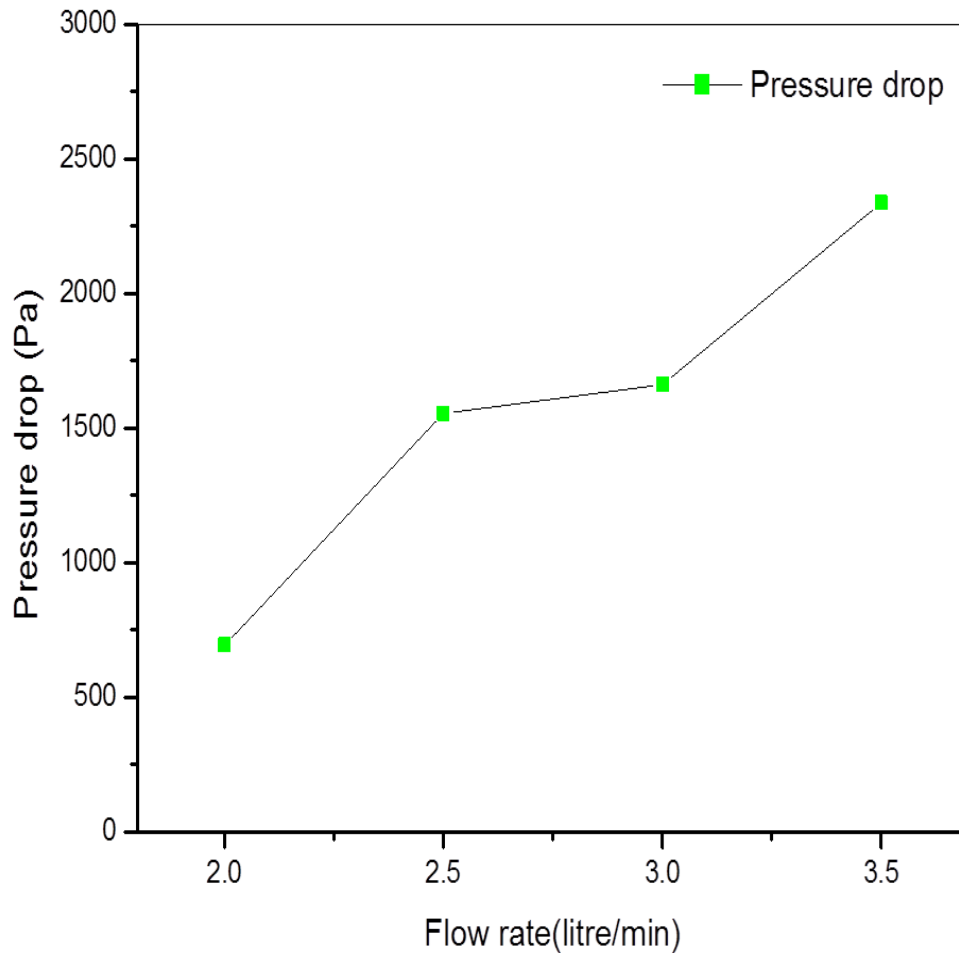


Figure 4.1: Flow Rate against Pressure Drop

An experiment to measure pressure drop has been conducted by using distilled water under flow rate of 2.0 litre per minute to 3.5 litre per minute. The figure 4.1 shows the pressure drop against flow rate from 2.0 litres per minute to 3.5 litre per minute at time 9 AM.

Based on the Figure 4.1, the result shows that with the increase of flow rate the pressure drop will increase. The results obtained are in good agreement with Foster R.et

al (2010). Foster R. et al have investigated that higher flow rate contribute to greater pressure drop. The minimum pressure drop of the figure is 694 Pa which is at flow rate 2.0 litre per minute and the maximum pressure drop is 2336 Pa at flow rate 3.5 litre per minute.

There was a huge increment of pressure drop at flow rate 3.5 litre per minute which is from 1661 Pa at 3.0 litre per minute to 2336 Pa. Flow rate 3.5 litre per minute is not suitable flow rate for the system it because excessive pressure drop will lead to poor results in system performance. Besides that excessive pressure drop will increase the power consumption and this will lead to decreased of efficiency of the system. This satisfy with the what has been reported by Steve P. S, (2010).

Besides that an important fundamental relationship for the duct fluid that runs in the collector using Fanning equation where $\Delta P = \frac{4 f W^2 L}{2 g A^2 \rho D}$ which is W is the flow rate (Elradi A. M. et al, 2004). From the equation if the flow rate is increase the pressure drop will increase and this are in agreement with the results shown in the figure 4.1.

4.2.3 Performance Analysis Of Pressure Drop at Different Temperature

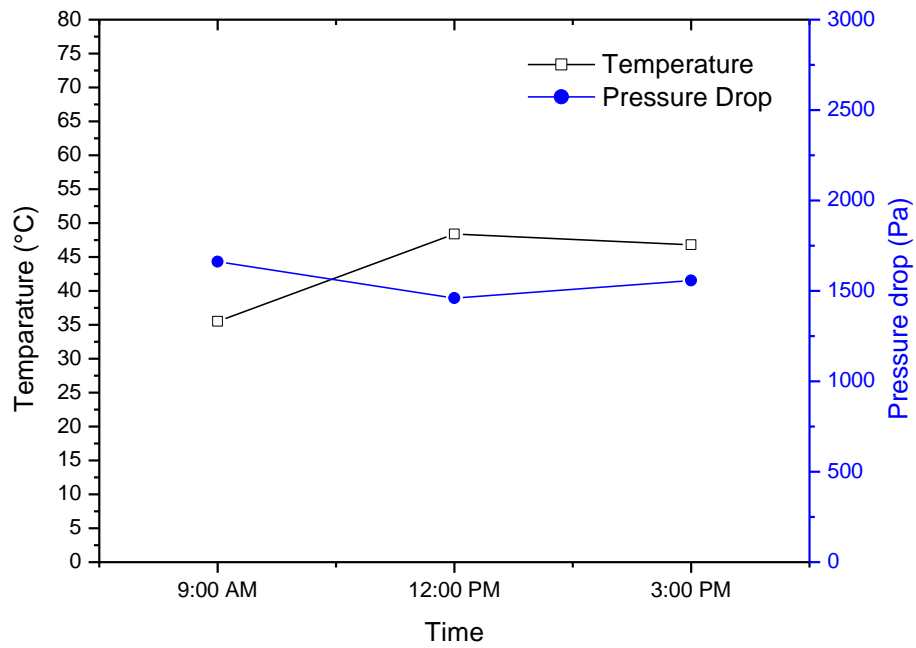


Figure 4.2 :Time against Temperature and Pressure Drop

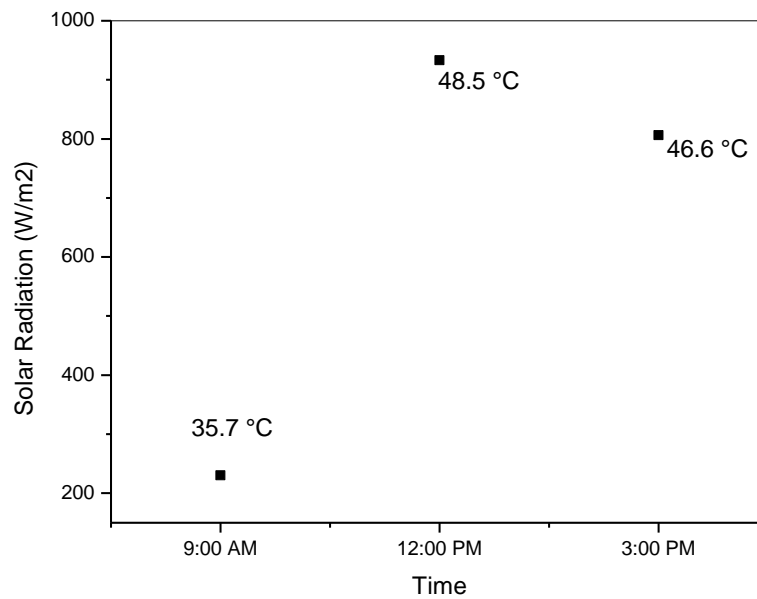


Figure 4.3 :Time against Solar Radiation

Figure 4.2 shows time against temperature and pressure drop. The readings were taken at 9 am, 12 pm and 3 pm. The readings of pressure drop was take at three different time to differentiate the temperature which is based on the figure shows above at 9 am the temperature is 35.5 °C . The temperature is increase at afternoon which is as we can see in the figure above at 12 pm the temperature increase to 48.4 °C and the temperature decrease at 3 pm to 46.8 °C. There was drop in temperature at 3 pm because of a cloud factor. In the present experiment, weather conditions such as passing cloud, cloudy sky, rain and etc influence the temperature and solar insolation values. Figure 4.3 shows the solar insolation against time. Solar radiation shows the increment as the temperature increase as shown in figure 4.3. Solar radiation was highest at 12.00 pm which is at that time the temperature is highest.

As clearly demonstrated in figure 4.2, 4.4, 4.5, 4.6, as the temperature increased the pressure drop will decreased and this results satisfy with have been reported by Albanakis C. et al (2009). With the higher temperature, the resistance to flow is lower which mean the viscosity is decreased. As the viscosity decreased the pressure drop also will decreased (Elradi A. M et al, 2004). As can be seen in figure 4.2 at 9 am the temperature is 35.5 °C and pressure drop is 1661 Pa and at 12 pm the temperature increased to 48.4 °C and the pressure drop decreased to 1460 Pa and this results are in good agreement with the report by Elradi A. Musa (2004).

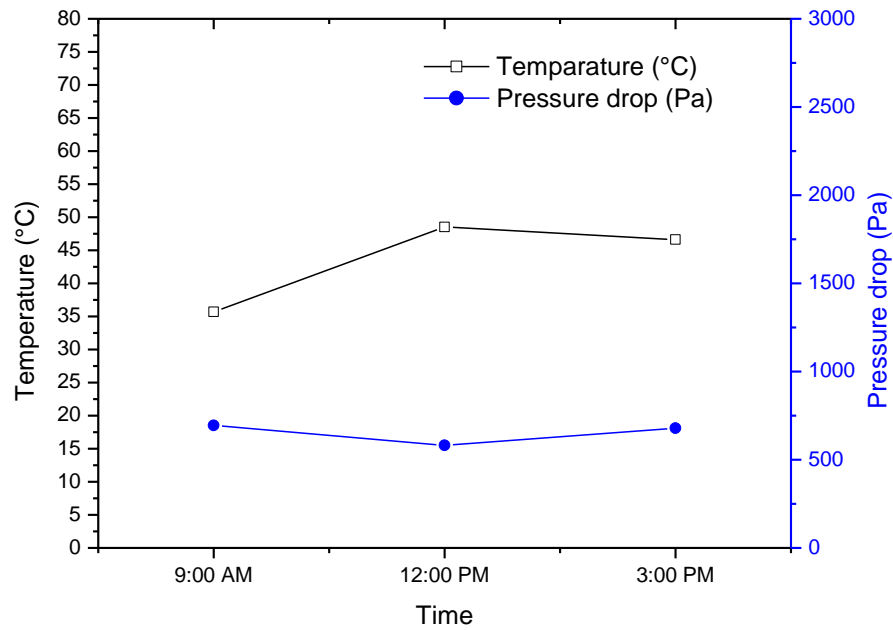


Figure 4.4 :Time against Temperature and Pressure Drop (2 litre per minute)

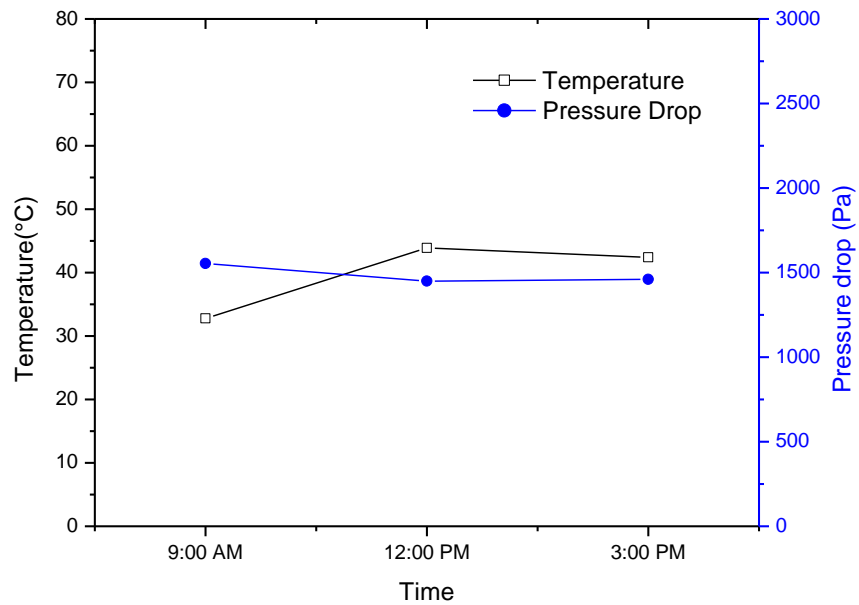


Figure 4.5: Time against Temperature and Pressure Drop (2.5 litre per minute)

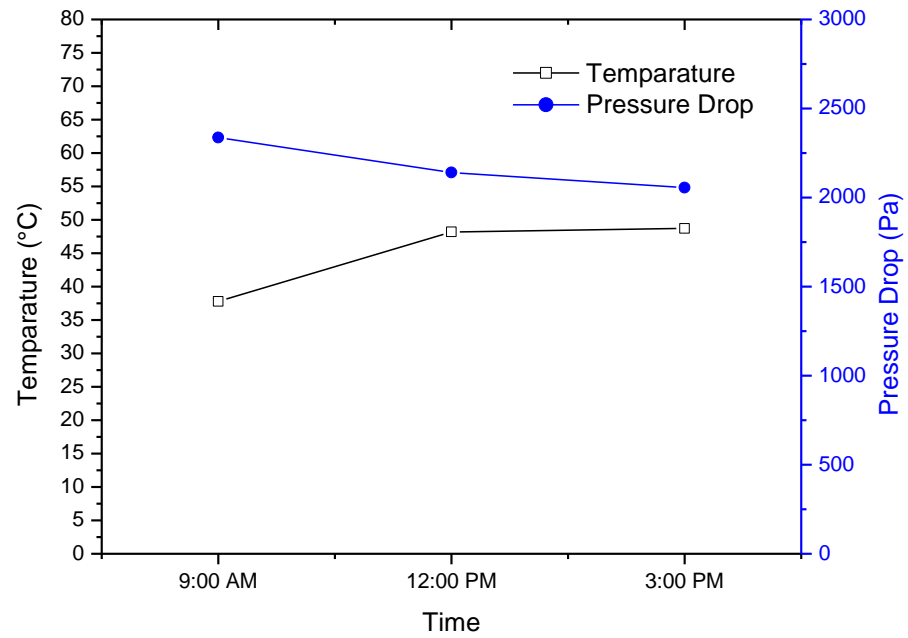


Figure 4.6 : Time against Temperature and Pressure Drop (3.5 litre per minute)

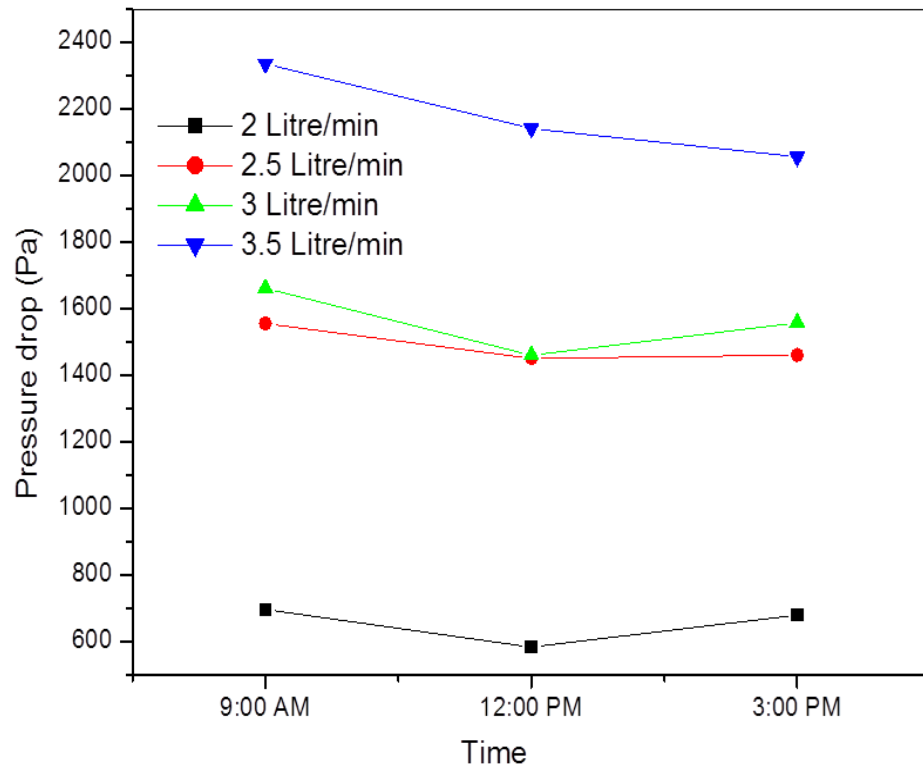


Figure 4.7 : Pressure Drop against Time

The above figure 4.7 shows pressure drop against time from flow rate 2.0 until 3.5 litre per minute. As seen from figure 4.7 above, the pressure drop for all the flow rate was quite stable and there is not much difference between the readings at 3 pm and 9 am. As discuss based on the figure 4.2 before , there was drop in pressure drop at 12 pm and the pressure drop increase back at 3 pm. This happen because of the relation between temperature and pressure drop as discuss before. There was increase of temperature at 12 pm and at 3 pm the temperature drop it can be caused by the cloud or wind factor

Based on the graph in the figure 4.7 percentage difference in the pressure drop from 9 am to 3 pm for flowrate 2 litre per minute is 2 %. For flowrate 2.5 litre per minute 7 %, 3 litre per minute 6 % and 3.5 litre per minute is 12 %. Based on this percentage of difference it can be said that at flow rate 2.5 litre per minute the readings

of pressure drop is the most stable because there is not much difference in the readings which is only 2 % .

Sample Calculation for Percentage of Difference of Pressure Drop at 2 litre per minute

$$\begin{aligned}\text{Percentages of Difference} &= \frac{(\text{Reading at 3 PM} - \text{Reading at 9 AM})}{(\text{Reading at 9AM})} \\ &= \frac{(694 - 678)}{678} \\ &= 0.02 \\ &= 2 \%\end{aligned}$$

4.3 PERFORMANCE ANALYSIS OF PRESSURE DROP FOR NANOFLUID (SiO₂) AT SOLAR SYSTEM

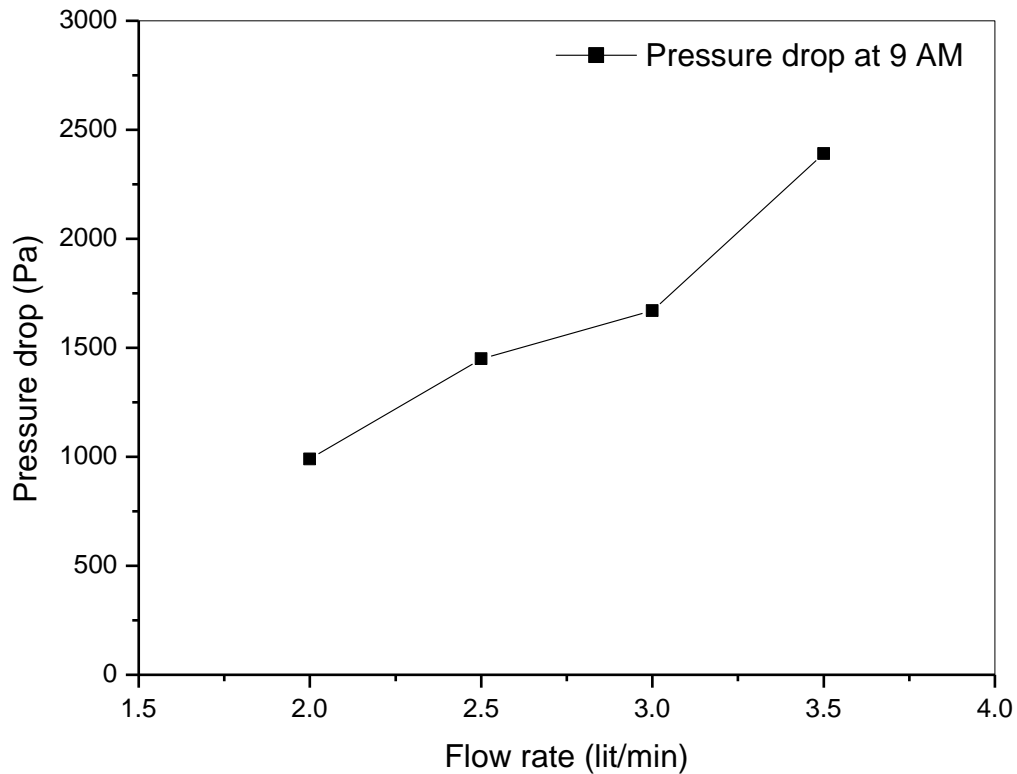


Figure 4.8 : Flow rate vs Pressure drop for nanofluid (SiO₂)

An experiment to measure pressure drop has been conducted by using nanofluid (silicon oxide) under flow rate of 2.0 litre per minute to 3.5 litre per minute. The above figure 4.8 shows the pressure drop against flow rate from 2.0 litres per minute to 3.5 litre per minute at time 9 AM.

Figure 4.8 shown the trend of flow rate versus pressure drop for flow rates 2.0 , 2.5 ,3.0 , and 3.5 litre per minute. As seen from figure 4.8, it is apparently that the pressure drop increase with an increase in flow rate. The minimum pressure drop within the range of the experiment based on the figure is 989 Pa which is at flow rate 2.0 litres per minute and the maximum pressure drop is 2390 Pa at flow rate 3.5 litre per minute.

As in experiment with distilled water pressure drop is increase as flow rate increased. A similar trend of result is get for experiment with nanofluid. As discussed earlier in Section 4.2.2, Foster R. et al (2010) have investigated that higher flow rate contribute to greater pressure drop. As flow rate increase, the movement of nanoparticles suspended in fluid is strengthens which mean the movement between one particle to another particles is more harder. Besides, the collision of nanoparticles also strengthens as flow rate increase. These factors contribute to higher pressure drop in the system. More collision and movement in the tube will cause resistance to fluid flow and cause pressure drop increase (Teng T. P et al ,2011) .

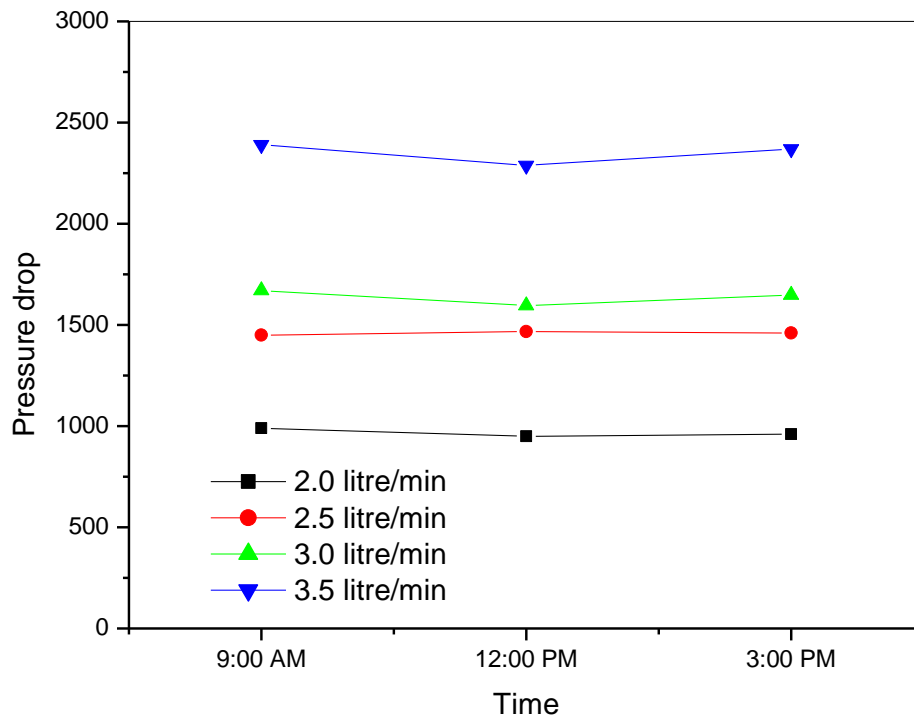


Figure 4.9: Pressure Drop against Time for nanofluid (SiO₂)

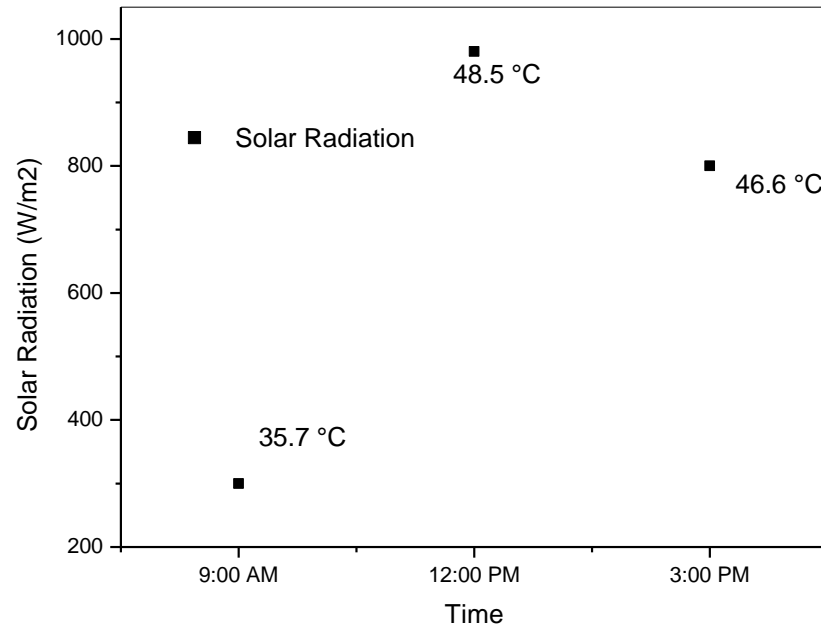


Figure 4.10: Time Versus Solar Radiation for nanofluid

The figure 4.10 shows pressure drop against time from flow rate 2.0 until 3.5 litre per minute for nanofluid. As seen from figure 4.3, the pressure drop for all the flow rate was quite stable and there is not much difference between the readings at 3 pm and 9 am. The trend in the figure 4.8 is same with the trend in the Figure 4.7.

As discuss based on the figure 4.2 in the section 4.2.3, there was drop in pressure drop at 12 pm and the pressure drop increase at 3 pm because of the relation between temperature and pressure drop.

4.4 PERFORMANCE ANALYSIS OF DIFFERENCE OF PRESSURE DROP BETWEEN DISTILLED WATER AND NANOFLUID (SiO₂)

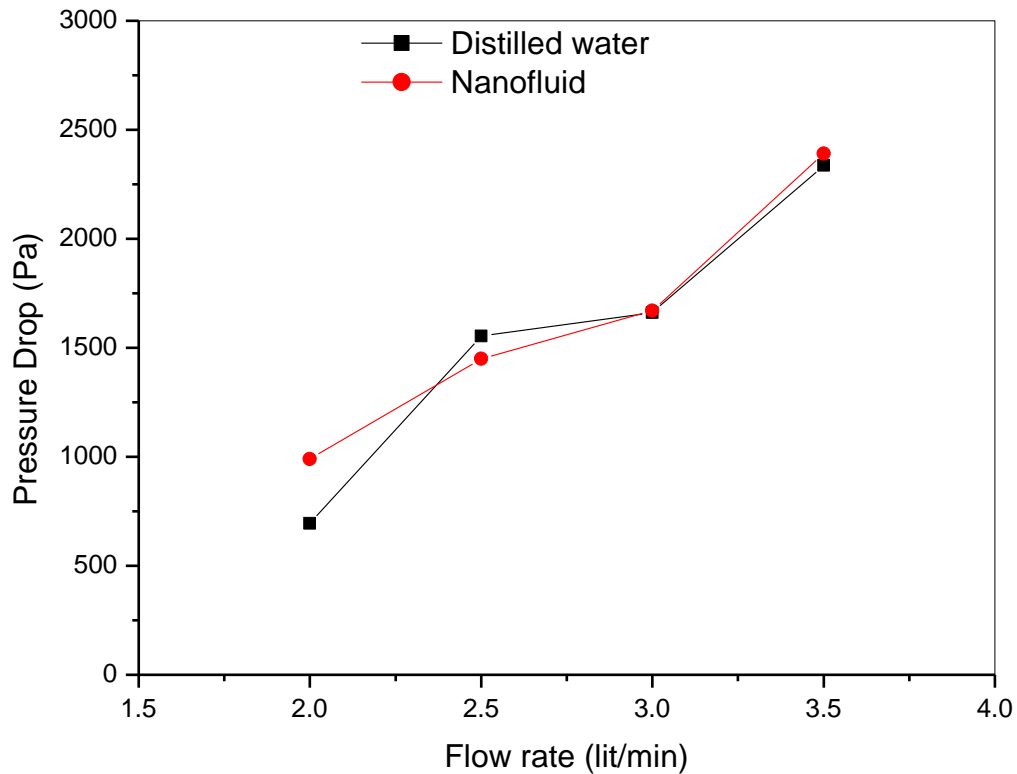


Figure 4.11 : Flow rate vs Pressure drop for distilled water and nanofluid

Figure 4.11 shown the trend of flow rate versus pressure drop for two working fluid, distilled water and nanofluid (silicon oxide).As seen from figure above, for both working fluid the pressure drop is increase as the flow rate increase. The minimum pressure drop for both working fluids within the range of this experiment is at flow rate 2.0 litre per minute. For distilled water the maximum pressure drop is at 3.0 litres per minute. The same trend is obtained for the nanofluid which is the maximum pressure drop at flow rate 3.0 litre per minute.

As observed in the figure 4.11, pressure drop with nanofluid is more higher than pressure drop without nanofluid. Figure 4.11 shows the pressure drop of SiO₂ nanofluid

is higher than distilled water, where the maximum pressure drop for this experiment was 2369 Pa and 2056 Pa respectively.

As discuss before in the section 4.2.3, Elradi A. M et al, (2004) have investigated that as the viscosity decreased the pressure drop also will decreased. Suspension of nanoparticles in the base fluid causes the viscosity of nanofluid increase and from this it can be conclude that nanofluid is more viscous than distilled water. As the viscosity increase the pressure drop will increase. This satisfy with result shown in the figure 4.7 above which pressure drop of nanofluid is more higher than distilled water.

Nanofluid is a fluid containing nanometer called nanoparticles (Wenhua Yu ,2009). Wenhua Yu have investigated that combination of nanoparticles in liquid had increase the friction. Combination of nanoparticles causes an increase of viscosity and as viscosity increase the friction will increase. Hence as the friction increase the pressure drop will increase. The results obtained shown that at most of the flow rate nanofluid give higher pressure drop than distilled water. The result obtained are in good agreement with Wenhua Yu (2009).

In addition, fouling effect is also one of the factor that contribute to higher pressure drop to nanofluid. Fouling is a formation of nanoparticles on the surfaces. The formation of nanoparticles on the tube surfaces like in the figure 4.12 below causes an increase of friction due to increase of surface roughness. As the friction increase the pressure drop will increase. This satisfy with result as shown in the figure 4.7 , where the nanofluid contribute to the higher pressure drop compared to the distilled water.



Figure 4.12: Fouling Effect

4.5 SOLAR COLLECTOR EFFICIENCY PERFORMANCE ANALYSIS

4.5.1 Efficiency of Evacuated Tube Solar Collector without Nanofluid

The performance of the solar collector was evaluated experimentally by calculating the efficiency of the solar collector by using the equation 2.1 which is

$$\eta = \dot{m} C_p (T_{\text{out}} - T_{\text{in}}) / A_c G$$

where the value of C_p is different for different temperature. The efficiency of solar collector is calculated by using the C_p as shown in the table below.

Table 4.2: Specific Heat Capacity at Different Temperature

TEMPERATURE (°C)	SPECIFIC HEAT CAPACITY (kJ/kgK)
30	4179
35	4178
40	4179
45	4181
50	4182
55	4183
60	4185

Source: Sohel (2011)

Sample Calculation for Efficiency of ETSC (2.5 litre per minute at 12 pm)

$$\begin{aligned} \eta &= \dot{m} C_p (T_{out} - T_{in}) / A_c G \\ &= (2.5 / 60) (4182)(49.4 - 41.7) / (906) (3.708) \\ &= 0.40 \\ \eta &= 40 \% \end{aligned}$$

Table 4.3 : Relationship Between Pressure Drop and Time with Solar Collector Efficiency for Distilled Water

Flow rate	Time	Pressure Drop (Pa)	Solar Collector Efficiency (%)	Percentage of Change (%)
2	9:00 AM	694	95	94
	12:00 PM	582	49	
	3:00 PM	678	51	
2.5	9:00 AM	1554	55	38
	12:00 PM	1450	40	
	3:00 PM	1460	52	
3.0	9:00 AM	1661	38	52
	12:00 PM	1460	41	
	3:00 PM	1557	27	
3.5	9:00 AM	2336	27	107
	12:00 PM	2141	46	
	3:00 PM	2056	56	

Based on the table 4.3 it can be conclude that at flow rate 2.5 lit/min the efficiency of ETSC is most stable which is as shown in the table 4.3, the percentage of change of the solar collector efficiency is lowest at flow rate 2.5 lit/min.

At flow rate 2, 3.0, 3.5 lit/min the solar collector efficiency is quite unstable. As shown in table 4.3, solar collector efficiency at flow rate 3.5 lit/min was the most unstable. Solar insolation is one of the factors that contribute to the unstable solar collector efficiency. Low solar insolation caused an increase of the solar collector efficiency and contributes to the unstable efficiency. Cloud and wind factor was one of the factors that caused a drop in solar insolation.

4.5.2 Efficiency of Evacuated Tube Solar Collector with Nanofluid

Determination of Specific Heat Capacity of Nanofluid

The specific heat of capacity of nanofluid is calculated by using the Eq 4.1 (Zhou et al.(2010))

$$C_{nf} = \frac{(1-\phi)(\rho C)_w + \phi(\rho C)_p}{(1-\phi)\rho_w + \phi\rho_p} \quad (4.1)$$

The density of nanoparticle and specific heat of particles is take from Table 3.1

Sample Calculation of specific heat of capacity

$$C_{nf} = \frac{(1-\phi)(\rho C)_w + \phi(\rho C)_p}{(1-\phi)\rho_w + \phi\rho_p}$$

$$C_{nf} = \frac{(1-0.02)(1000*4181)+(0.02)(2220*745)}{(1-0.02)(1000)+(0.02*2220)}$$

$$C_{nf} = 4032$$

Sample calculation

Sample Calculation for Efficiency of ETSC (2.0 litre per minute at 9 am)

$$\eta = (m) C_p (T_{out} - T_{in}) / A_c G$$

$$= (2.0 / 60) (4032)(37.5 - 34) / (3.708) (300)$$

$$= 0.40$$

$$\eta = 40 \%$$

Table 4.4 : Relationship Between Pressure Drop and Time with Solar Collector Efficiency for SiO₂ Nanofluid

Flow rate	Time	Pressure Drop (Pa)	Solar Collector Efficiency (%)	Percentage of Change (%)
2	9:00 AM	989	42	23
	12:00 PM	950	43	
	3:00 PM	960	35	
2.5	9:00 AM	1450	33	73
	12:00 PM	1467	46	
	3:00 PM	1460	57	
3.0	9:00 AM	1670	97	54
	12:00 PM	1596	70	
	3:00 PM	1647	63	
3.5	9:00 AM	2390	70	4
	12:00 PM	2289	68	
	3:00 PM	2369	67	

Based on the table 4.4 percentages of change of solar collector efficiency at flow rate 3.5 lit/min is the lowest. Even though at flow rate 3.5 lit/min percentage of change is lowest, the solar collector efficiency at 3.5 lit/min is quite unstable. The stable solar collector efficiency is in the range of 40-55 %. As shown in the table 4.4, the solar collector efficiency at flow rate 3.5 lit/min is in range 67-70 %. This has proved that solar collector efficiency at flow rate 3.5 lit/min was not stable . .

CHAPTER 5

CONCLUSION AND RECOMMENDATION

5.1 CONCLUSION

The objective of this project have been fulfilled. The pressure drop system for solar collector had successfully set up. With the pressure drop system, the data for pressure drop were collected by recorded the height of a column of distilled water and silicon oxide. Solar radiation increase as the temperature increase. The analysis on the pressure drop system for ETSC had shown that as the temperature increase the pressure drop will decrease for both working fluid, SiO₂ nanofluid and distilled water.

Flow rate can affect the performance of the pressure drop. Pressure drop will increase as the mass flow rate increase for both working fluid.

Addition of nanoparticle to the base fluid had make pressure drop of the SiO₂ nanofluid higher than distilled water. As it was proved by the analysis in this report pressure drop of the nanofluid is more higher than distilled water. Maximum pressure drop with and without nanofluid was 2369 Pa and 2056 Pa respectively.

5.2 RECOMMENDATION

For future research and development on the pressure drop system for ETSC;

- I. Need to varies the flow rate not only until 3.5 litre per minute so that can get the bigger range of pressure drop and can get the optimum value of pressure drop.
- II. In order to know which nanofluid is more better as the working fluid at pressure drop system and what concentration is suitable for system type of nanofluid and concentration of nanofluid need to be varies.
- III. Pressure transducer can be used to obtain more accurate result of pressure transducer.
- IV. Recorded the result for one hour time interval so that can analyse the pressure drop with more range of temperature.

REFERENCE

- Albanakis, C., Missirlis, D., Michailidis, N., Yakinthos, K., Goulas, A., Omar, A., Omar, H., Tsipas, D., Grainer B. (2009). Experimental analysis of the pressure drop and heat transfer through metal foams used as volumetric receivers under concentrated solar radiation. *Experimental Thermal and Fluid Science*. **33**:246-252.
- A.H. Battez, R.G. alez, J.L. Viesca, J.E. Fernandez, J.M. Diaz Fernandez, A. Machado, R. Chou, J. Riba, CuO, ZrO₂ and ZnO nanoparticles as antiwear additive in oil lubricants, *Wear* 265 (2008) 422–428
- Azhar Ghazali, M., Abdul Rahman, A.R. 2012. The Performance of Three Different Solar Panels for Solar Electricity Applying Solar Tracking Device under the Malaysian Climate Condition. *Energy and Environment Research* .**2** (1) : 235-243
- Azhari, A.W. ,Sopian, K. ,Zaharim, A. ,Al Ghoul ,M. 2008. A New Approach For Predicting Solar Radiation In Tropical Environment Using Satellite Images – Case Study Of Malaysia. **4** :373-378
- Elradi, A.M.,Sopian, K.,Abdullah ,S.(2004).Heat transfer analysis and pressure drop correlation for the double-pass solar collector with porous media.**3**:15-24
- Izadi, M. , Hossainpour, S., Vahid, D.J.,(2009), Effects of Nanolayer Structure and Brownian Motion of Particles in Thermal Conductivity Enhancement of Nanofluids, 3:4.
- Foster ,R. ,Ghassemi, M.,Cota, A. 2010.*Renewable Energy and the Environment*.Energy and Environment Series:Taylor & Francis Group
- John,A.D, William, A.B. 2006. *Solar Engineering of Thermal Process*.3rd ed:John Wiley & Sons,INC.
- Hayek, M., Assaf, F., Lteif, W. (2011). Experimental Investigation of the Performance of Evacuated-Tube Solar Collectors under Eastern Mediterranean Climatic Conditions. **6**: 618–626.
- Kalteh,M.,Abbassi, A.,Saffar-Avval,M.,Frinns, A.,Darhuber A.,Harting J.(2012). Experimental and numerical investigation of nanofluid forced convection inside a wide microchannel heat sink.**36** :260-268
- M.A. Akhavan-Behabadi, M.Ghazvini, E.Rasouli, Experimental investigation on heat transfer and pressure drop nano diamond-engine oil nanofluid in a microfin tube, IHTC14-22483,(2010)
- Morajevi,M.K.,Razvarz, S.(2012).Eperimental investigation of aluminium oxide nanofluid on heat pipe thermal performance.**39**:1444-1448

- Morrison, G.L.,Budihardjo,I.,Behnia M.(2004) Water-in-glass evacuated tube solar water heaters. **76** :135–140
- Murshed ,S.M.S. ,Leong, K.C.,Yang, C.(2009). A combined model for the effective thermal conductivity of nanofluids.**29**: 2477–2483
- Nasiri,M.,Etemad, S.Gh.,Bagheri, R.(2011).Experimental heat transfer of nanofluid through an annular duct.**38**:958-963.
- Pirhayati, M., Akhavan, M. A.,Behabadi, Khayat, M.,2012, PRESSURE DROP OF CUO-BASE OIL NANOFLUID FLOW INSIDE AN INCLINED TUBE, 2231-1963.
- Pressure Transducer Basics - A Primer.(Online) access 22 NOVEMBER 2012 (http://www.aeroconsystems.com/electronics/Pressure_transducer_basics/Transducer_primer.htm)
- Saidur, R.,Leong, K. Y.,Mohamad, H.A.(2011). A review on application and challenges of nanofluids.**15**:1646-1668.
- Saidur,R.,Ghadini, A.,Wetselar ,H.S.C.(2011). A review of nanofluid stability properties and characterization in stationary conditions. **54** :4051–4068.
- Sharma, K.V.,Syam Sundar,L.(2010).Heat Transfer Enhancement of Low Volume Concentration Al₂O₃ nanofluid and with Longitudinal Strip Insert in a Circular Tube.**53**:4280-4286.
- Sohel Murshed S. M. and Nieto de Castro C. A.,2011, Contribution of Brownian Motion in Thermal Conductivity of Nanofluids,3: 6 - 8
- Soteris, A.K.2004. Solar thermal collectors and applications. **30** :231–295
- Specification of Digital Overhead Stirrer. (online). 16 OCTOBER 2012 (http://www.ika.com/ika/product_art/manual/ika_rw_20_d.pdf)
- Steve, P. S., Garron, K. M.(2010). Nanofluids in a Forced-Convection Liquid Cooling System Benefits and Design Challenges . **978(1)**:4244-5343.
- Tiwari, G.N. 2004.Solar Energy, Fundamental, Design ,Modelling and Application,Alpha Science International Ltd,Pangbourne England.
- Wenhua Yu,David, M. F. ,David S.S.,Singh, D.,Elena, V.T.,Jules,L.R.(2009). Heat Transfer to a Silicon Carbide/Water Nanofluid.*International Journal of Heat Transfer and Mass Transfer* .**52**:3606-3612
- Wenhua Yu,David, M.F.,David, S.M.,Dileep,S.,Elena,V.T.,Jules, L.R.(2009).Heat transfer to a silicon carbide/water nanofluid.**52**:3606-3612.

Specification of Digital Overhead Stirrer. (online). 16 OCTOBER 2012
(http://www.ika.com/ika/product_art/manual/ika_rw_20_d.pdf)

